FAR FIELD WAKE VELOCITY MEASUREMENTS WITH HOT FILM PROBES.

By

Lewis Randall Grigg

B.S. Naval Architecture
U.S. Naval Academy (1981)

Submitted to the Department of
OCEAN ENGINEERING
In Partial Fulfillment of the Requirements
For the Degrees of

NAVAL ENGINEER

and

MASTER OF SCIENCE IN MECHANICAL ENGINEERING

at the

MASSACHUSETTS INSTITUTE OF TECHNOLOGY
June, 1990

A. Douglas Carmichael, Chairman
Departmental Graduate Committee
Department of Ocean Engineering

FAR FIELD WAKE VELOCITY MEASUREMENTS WITH HOT FILM PROBES.

by

Lewis Randall Grigg

Submitted to the Departments of Ocean Engineering and Mechanical Engineering
on May 11, 1990, in partial fulfillment of the requirements
for the degrees of Naval Engineer and Master of Science in Mechanical Engineering

ABSTRACT

An investigation into the feasibility of measuring wake velocity profiles in a towing tank using hot film probes has been conducted. Results show that such a system is feasible, but care must be taken to minimize calibration errors due to the small velocity differences being measured. Included are calibration data and plots of wake profiles behind a sphere measured at the U.S. Naval Academy's Hydromechanics Laboratory and the MIT Ship Model Towing Tank. These plots show the effect of the presence of a free surface on the development of a turbulent wake. Data collected using the hot film system can be used as an input to analytic wake algorithms, compared to wake prediction or visualization techniques.

Thesis Supervisor: Dr. Chryssostomos Chryssostomidis

Title: Professor of Naval Architecture

Thesis Reader: Dr. Triantaphyllos R. Akylas

Title: Associate Professor of Mechanical Engineering

Acknowledgements

In humility, I express my gratitude to the Lord Jesus Christ whose grace and power have given me the hope and strength to complete my studies at MIT.

I would like to thank Professor Chryssostomos Chryssostomidis and Dr. George Triantafyllou for their patience, encouragement and support in completing this thesis.

I would like to thank Professor Roger Compton and the staff at the U.S. Naval Academy Hydromechanics Laboratory, who granted me use of their facilities and gave so freely of their time.

Professor Joseph Haritonidis of MIT, Dr. Paul Temple of the Naval Underwater Systems Center, and Mr. Greg Reynolds of TSI Inc. were of great help, lending timely advice and encouragement.

I am grateful for the opportunity to attend MIT that was made possible by the U.S. Navy's strong support of my graduate education. In particular, the Office of Naval Research provided the funding that purchased the equipment used to complete this thesis.

My wife, Betty has blessed me with the great joys of a committed loving companion and two beautiful children. She is the greatest!

Table of Contents

List of Figures and Tables

Chapter 1:INTRODUCTION

1.1 Wake Detection

The problem of detecting ship wakes has received a great deal of attention in the past decade due to developments in ocean surveillance technology. "Seasat, an ocean-imaging satellite launched in 1978, revealed to the scientific community at large what Government investigators probably already knew: surface patterns associated with currents, seabed topography and internal waves many meters below the surface of the ocean can be imaged by a space-based microwave synthetic-aperture radar. ... Although the Seasat images confirmed that under some conditions synthetic aperture radar can detect modulations in ocean-surface roughness, the mechanism by which this occurs is not clearly understood."[1] Ship wakes many miles long have been observed in high sea states using synthetic-aperture radar[2] as well as infrared sensors. This thesis is part of a basic MIT research program to better understand the dynamics of ship wakes.

Rapid developments have already been made in computational analysis and prediction of wake characteristics and propagation.[3] Wake velocity measurements can be used as an input to analytic wake algorithms and compared to prediction and

---

[1]Tom Stefanick, "The Nonacoustic Detection of Submarines," Scientific American, March 1988, p. 46.

[2]For information on synthetic aperture radar see Charles Elachi, "Radar Images of the Earth from Space," Scientific American, December, 1982.

[3]G. S. Triantafyllou, "Three Dimensional Instability Modes of the Wake Far Behind a Ship" Proceedings, 18th ONR Symposium on Naval Hydrodynamics, Ann Arbor, MI, (1990), to appear.

visualization techniques of observable wake flows. This thesis demonstrates the feasibility of measuring far field average axial wake velocity profiles using an 8 channel, one dimensional, hot film probe system now available at the MIT Ship Model Towing Tank.

1.2 Basic Principles

The functional dependence of heat transfer from a heated wire on the properties of flow past it can be utilized to measure fluid velocity. This is the basic principle of operation of a hot wire anemometer. A heated sensor is held at a constant temperature using an electronic control circuit. Fluid flow past the sensor tends to cool it, so to maintain the temperature, a feedback circuit in the control electronics increases current to the sensor. The magnitude of the feedback, available as an output voltage, is directly related to heat transfer and, hence, to the flow causing it.[4]

Hot wire anemometry[5] has been used in the measurement of fluid flows since the late 1800's and is still found in research laboratories throughout the world. In general, hot wire probes can be used in a wide variety of liquid and gaseous fluids to measure speed, direction, and turbulence.

Hot wire anemometers have excellent sensitivity at low velocity, good spatial

---

[4]Hot Wire/Hot Film Anemometer Systems & Accessories, TSI Incorporated, St. Paul, MN 1985, p. 5.

[5]This nomenclature was developed in the early 1900's and is confusing as the name "hot wire anemometer" implies using a heated wire to make velocity measurements in the air. Today heated metal films are also used to make measurements in other fluids, but are often refer to as "hot wire anemometry".

resolution, and an output signal in the form of a voltage difference for convenient data analysis.[6] The combination of a small heated wire (low thermal mass) and anemometry electronics provides a fast response to changes in flow velocity. This instantaneous measurement of velocity can be utilized to calculate fluid mean velocity.

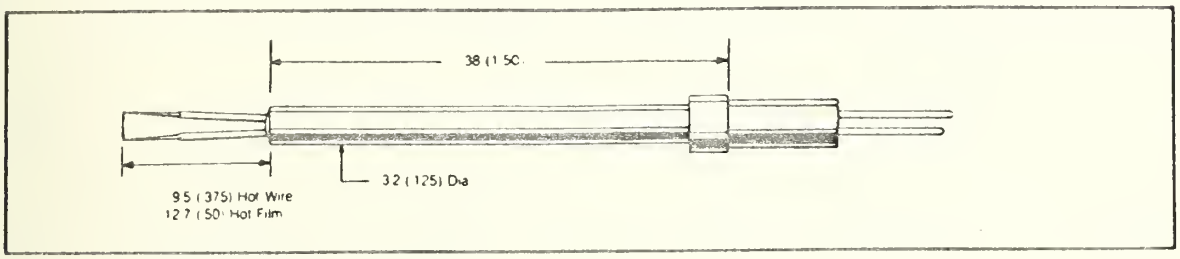

Figure 1.1. Typical hot film probe.

A typical hot film probe is shown in figure 1.1. It is usually made of a fused quartz substrate with a high purity platinum film bonded to the surface. Platinum is a stable, anticorrosive film material with the proper resistance characteristics for thermal anemometry. For liquid applications, the platinum film is coated with a thin layer of quartz to electrically insulate the sensor. Cylindrical film sensors are usually about .005" in diameter and cannot be easily seen with the unaided eye.

The resistance of the sensor is a function of temperature. A current is supplied to the sensor, which varies with the fluid velocity to maintain constant resistance and thus constant temperature. As shown in figure 1.2 the sensor is one resistor in a Wheatstone bridge circuit with three other fixed resistors, and controlled by a feedback amplifier.

The differential feed back amplifier senses any bridge imbalance and adds

---

[6]Charles G. Lomas, Fundamentals of Hot Wire Anemometry (New York: Cambridge University Press, 1986), p. 1.

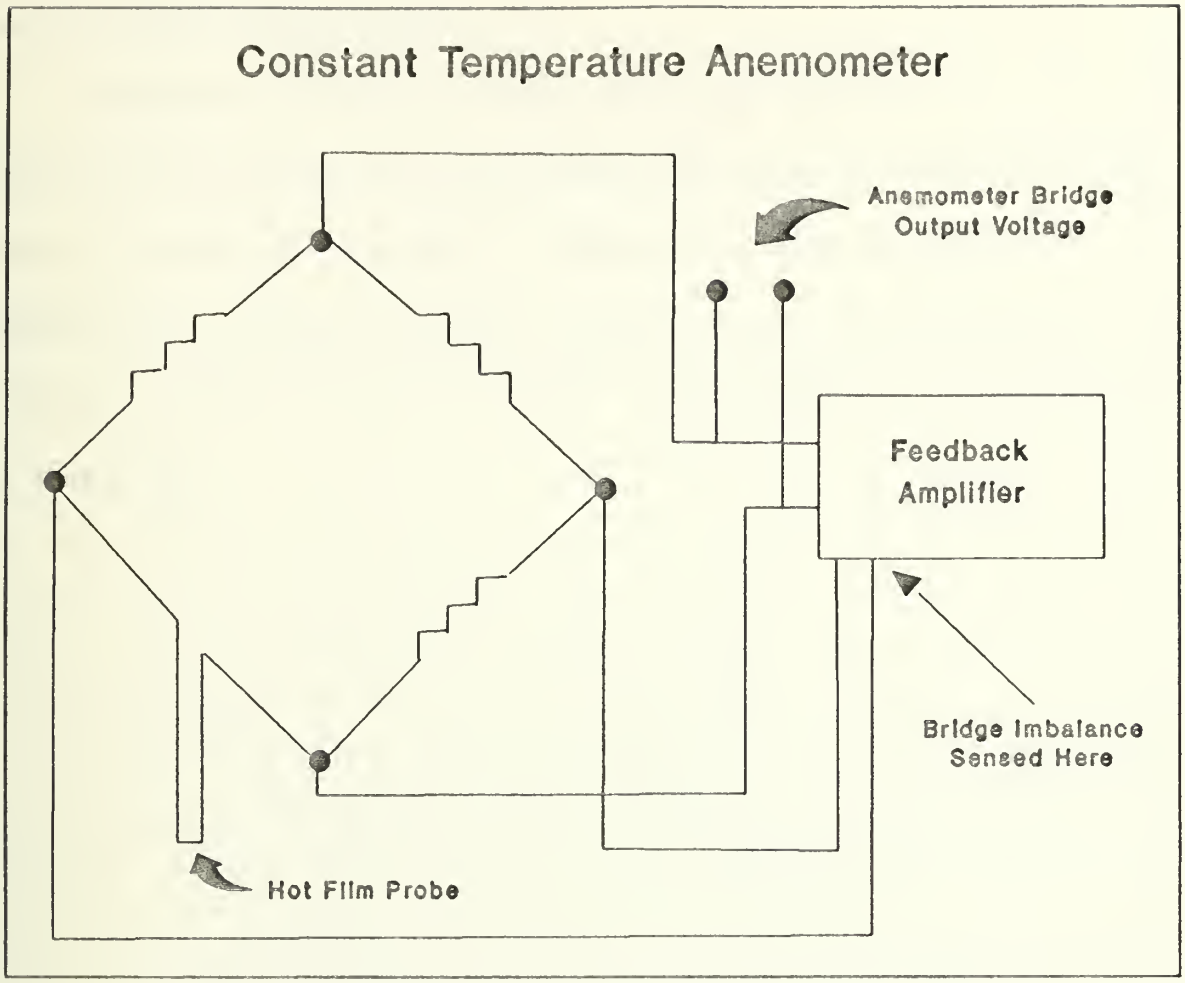

Figure 1.2. Anemometer diagram.

current to hold the sensor temperature constant. The resistor on the same leg as the sensor is of a value larger than would be required to balance the bridge when the system is turned off. When power is applied, the feedback amplifier increases the sensor heating current, causing the sensor temperature to rise and increase the sensor resistance until the bridge is balanced. A change in velocity will change the sensor resistance and unbalance the bridge. This causes the feedback amplifier to vary the sensor heating current and to bring the bridge back into balance. Since the feedback amplifier responds rapidly, the sensor temperature remains virtually

constant as the velocity changes.[7]

The application of hot film anemometry to the measurement of far field wake velocity profiles was chosen for the MIT Ship Model Towing Tank due to its proven success in other fluid flow experiments. Additionally, hot wire anemometry is compatible with existing data collection equipment, permits simple arrangements for simultaneous multiple channel data collection, and is significantly cheaper than laser based systems.

---

[7] Lomas, p. 3.

Chapter 2: EXPERIMENTAL PROCEDURE

This experiment was conducted with two objectives in mind. The first was to investigate the effectiveness of mapping the flow field in the far field wake using hot film probes in a towing tank. The second was to study the effect of the free surface in the development of a turbulent wake.

Data were collected at the U.S. Naval Academy's (USNA) Hydromechanics Laboratory and also MIT's Ship Model Towing Tank. Comparing the results between these two facilities will demonstrate how the unique characteristics of each facility influence the method of data collection and processing.

2.1 Equipment Setup

The equipment arrangement used to measure the wake profiles is shown in figures 2.1, 2.2, and 2.3. Photos of the setup are shown in figures 2.4, 2.5, and 2.6.

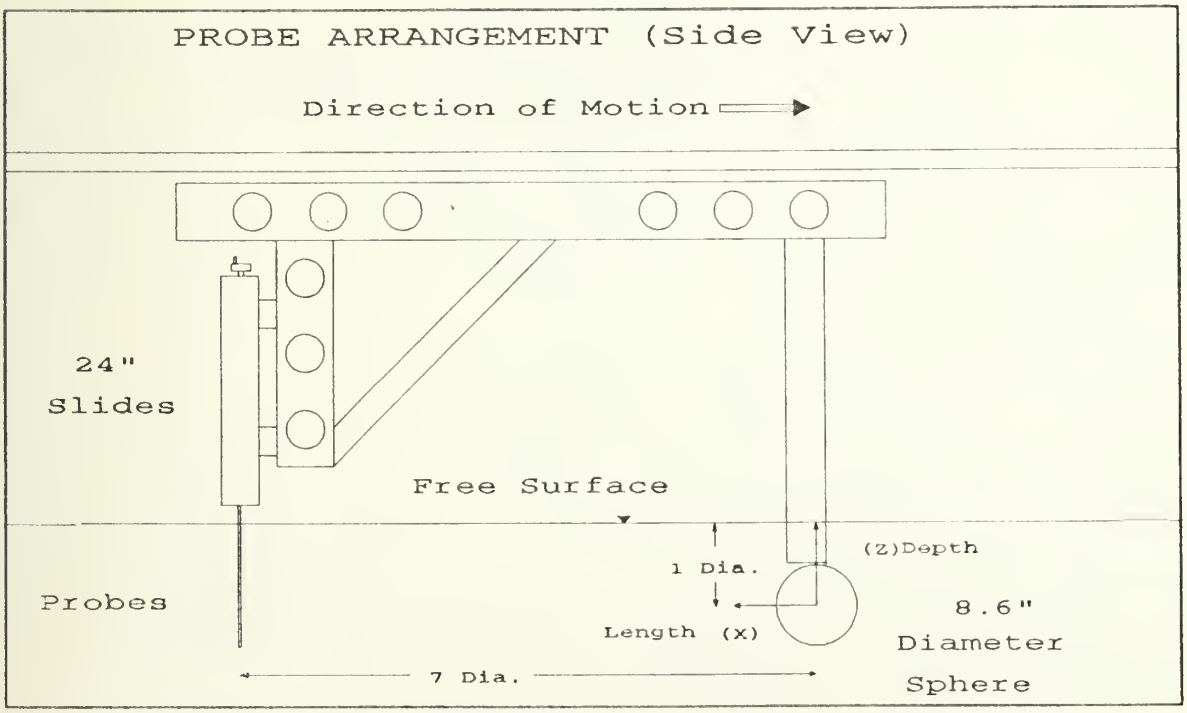

Figure 2.1 Experimental setup, side view.

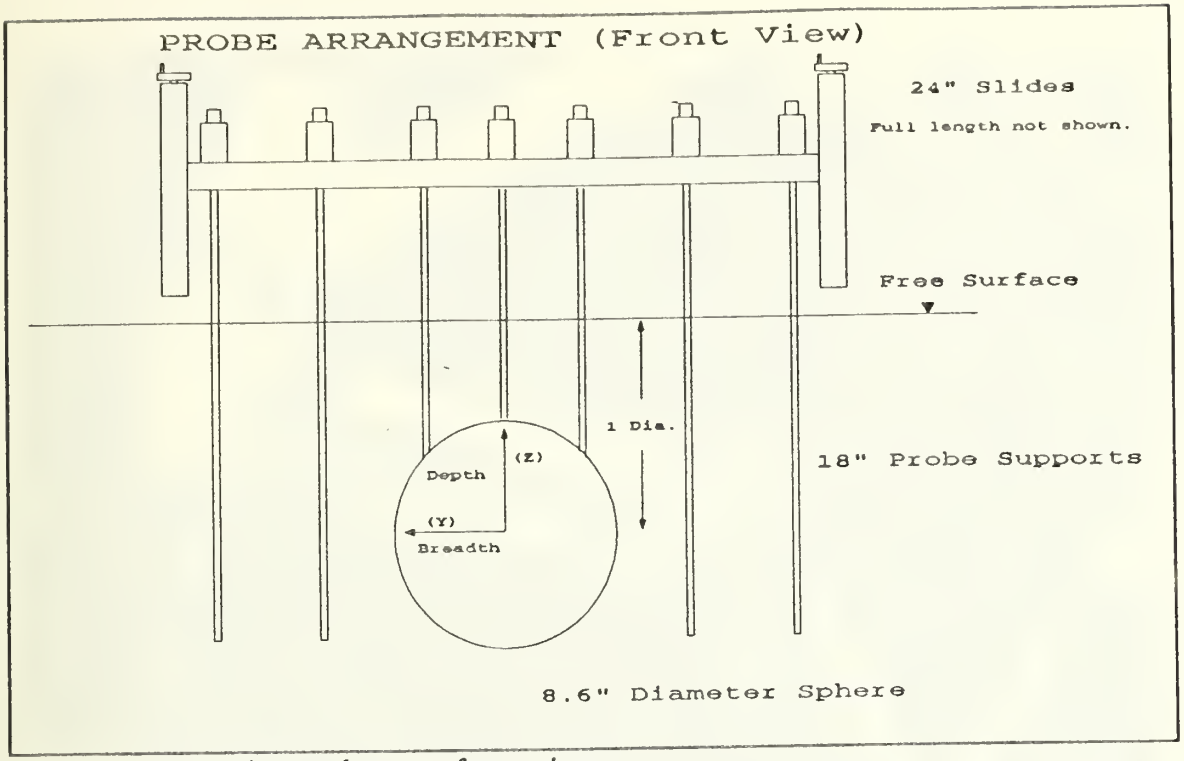

Figure 2.2 Experimental setup, front view.

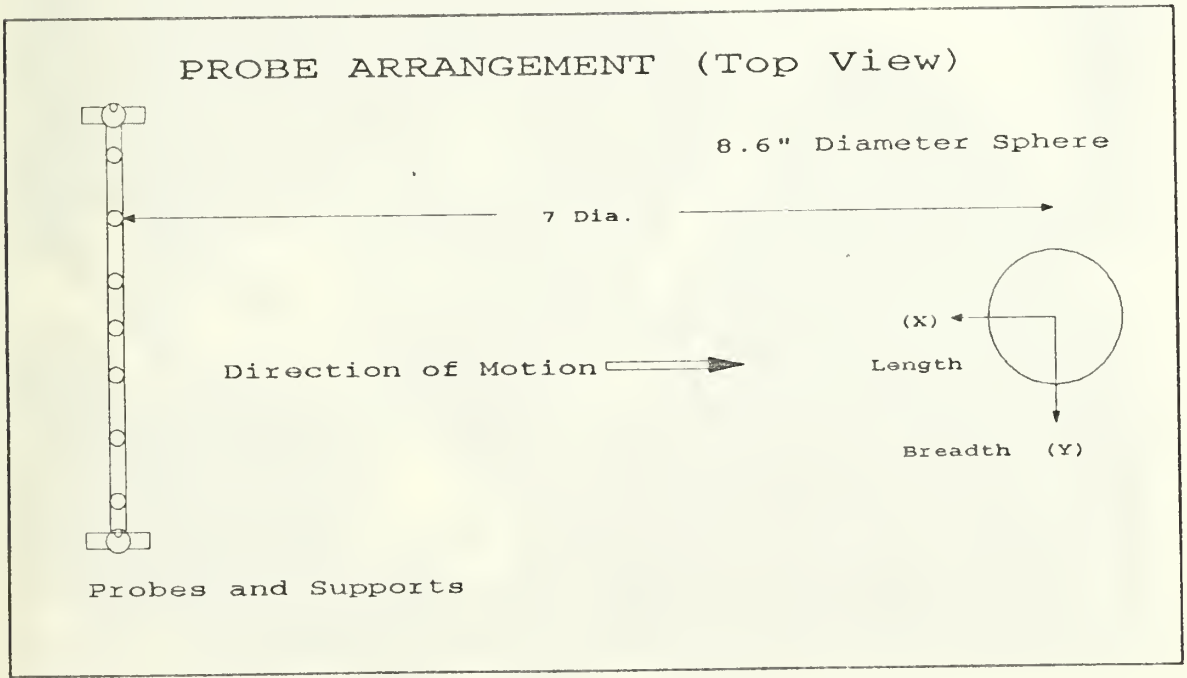

Figure 2.3 Experimental setup, top view.

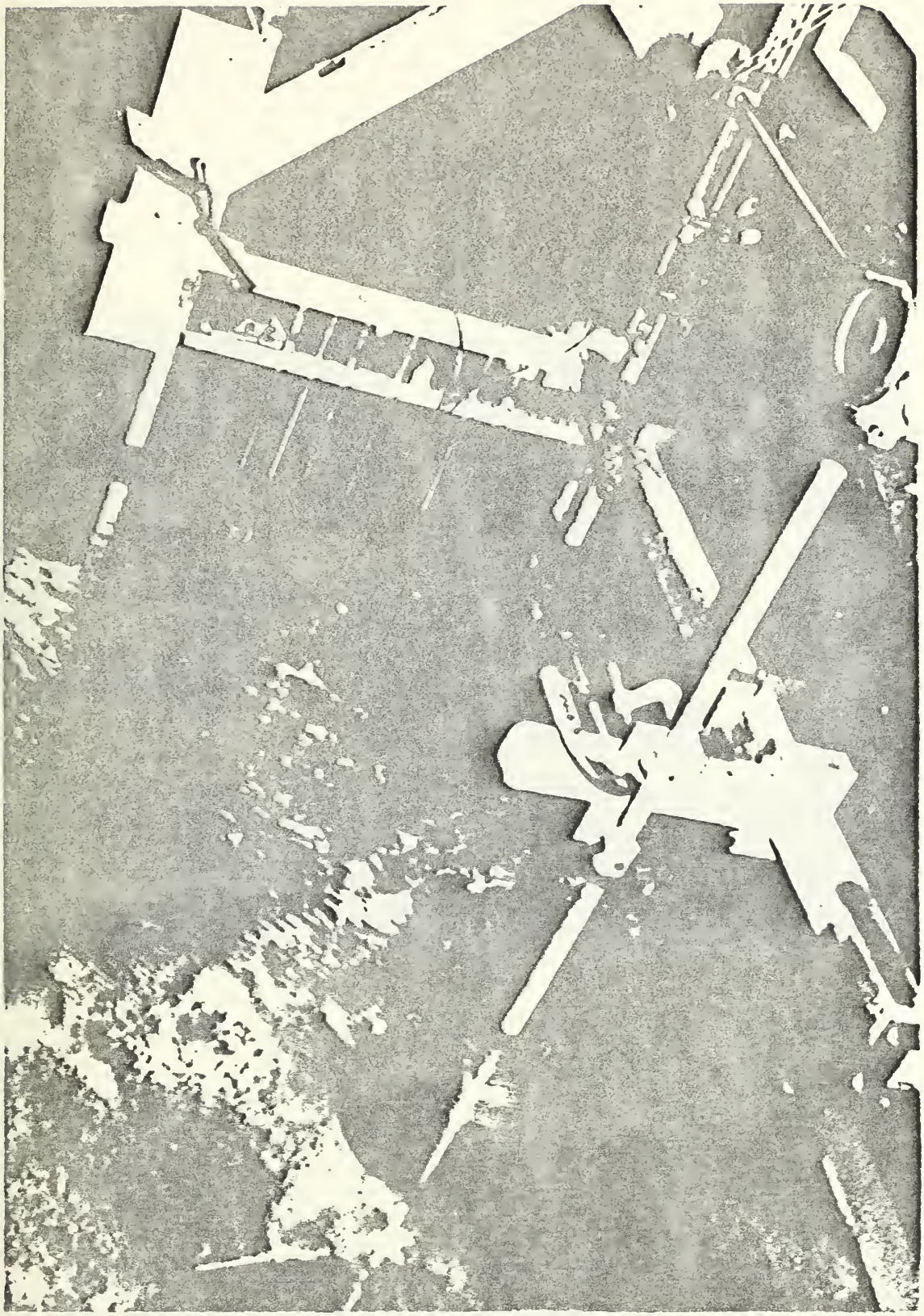

Figure 2.4 Top view of sphere and probes at USNA.

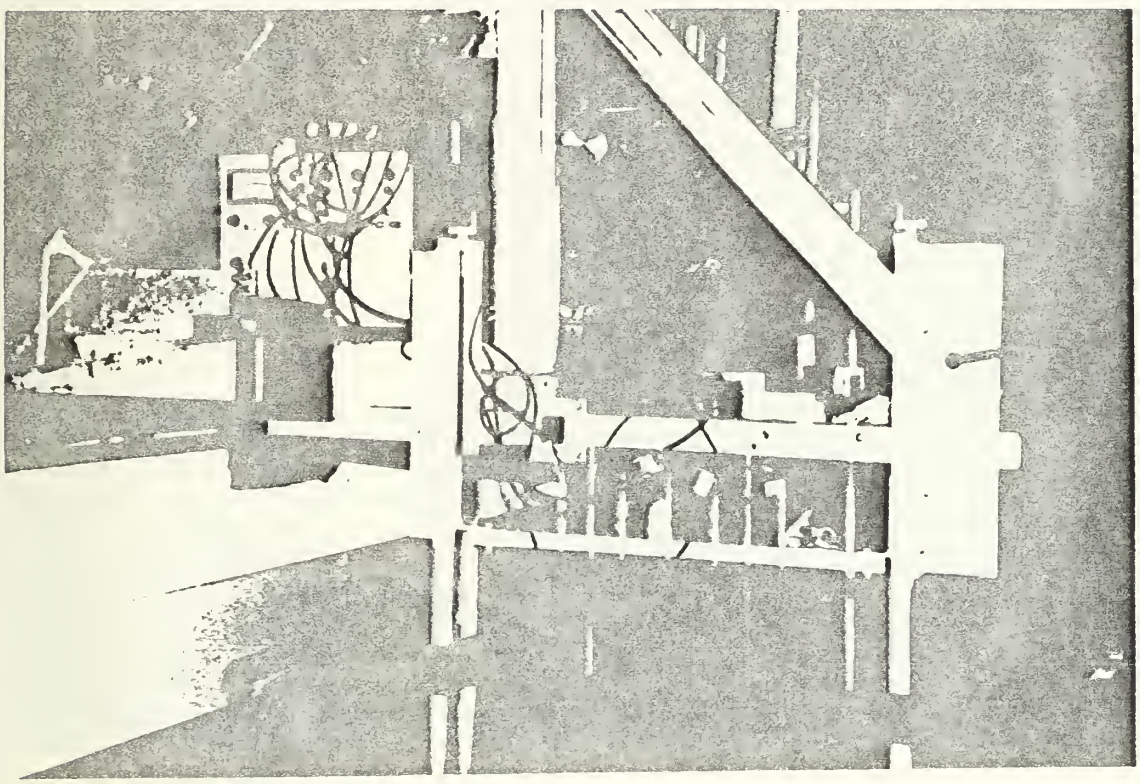

Figure 2.5 Anemometer and probe setup at USNA.

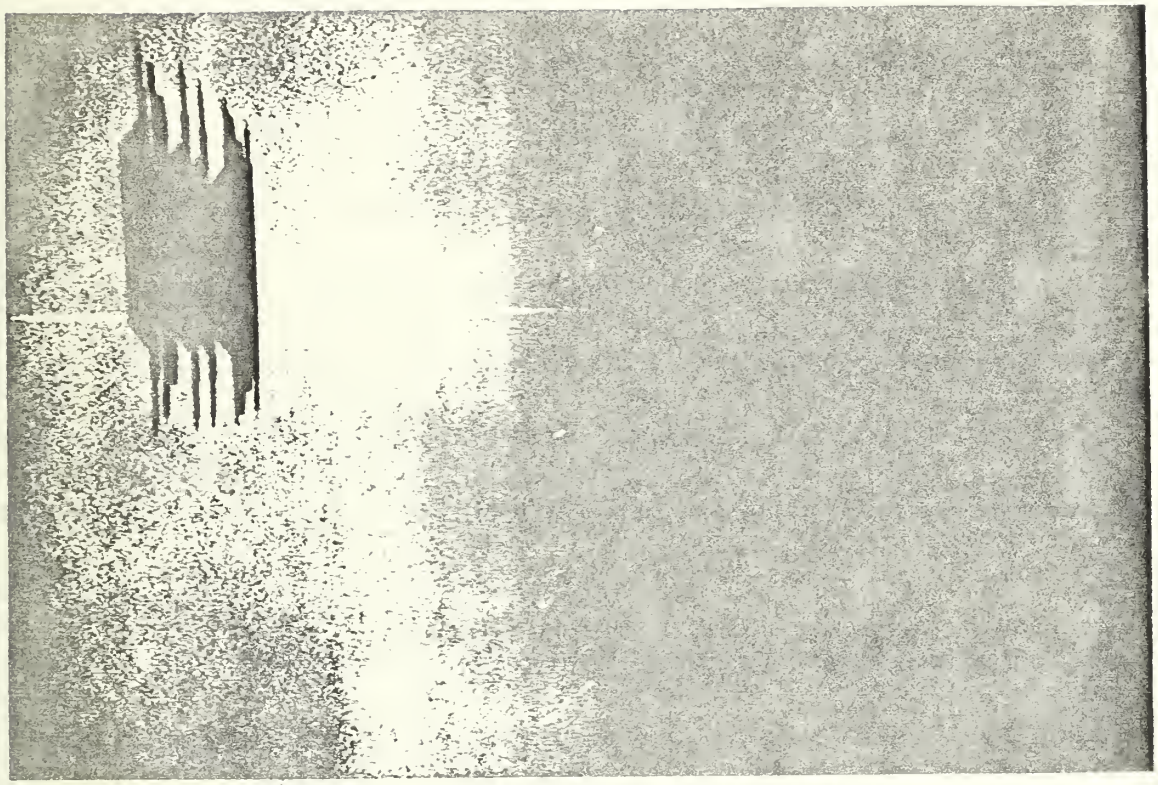

Figure 2.6 Underwater view of probes and sphere.

The wake behind a sphere at constant velocity in a homogenous fluid is symmetric about the centerline.[8] This symmetry was used to check the reliability of measurements obtained using hot film probes. The model was a standard 10 pin bowling ball. This sphere is smooth, manufactured to close tolerances and easily purchased. It's size of 8.6" in diameter allowed measurements to be taken at a Froude number below 0.2 and a Reynolds number above 10^4 (based on the diameter of the sphere) within the speed range of the towing tank. Thus, the Froude number is low, consistent with most applications, and the Reynolds number is fairly high to generate fully developed turbulence. A larger sphere would have made it difficult to mount the probes 5-7 diameters away without an elaborate carriage setup.

For most of the wake measurements the center of the sphere was submerged one diameter (8.6") below the free surface. The effect of the free surface is still present at this depth. Thus, symmetry is expected to exist in the wake only across a vertical plane and not across a horizontal plane.

The center of the sphere is used as a reference origin for the presentation and discussion of data throughout this thesis. Length is measured in the X direction, positive being aft of the sphere moving towards the probes. Breadth is measured horizontally in the Y direction, positive being to the left when looking down the wake past the sphere and towards the probes. Depth is measured vertically in the Z direction, positive being above the center of the sphere.

The hot film probes shown in figure 1.1 were mounted on the end of 18"

---

[8]Hermann Schlichting, Boundary-Layer Theory, 7th ed. (New York: McGraw-Hill Book Co., 1979) p. 743.

probe supports (see figure 2.2). The probe supports were attached to a 1" square aluminum bar suspended between two 24" long traversing slides. These slides permitted the probes to be moved vertically up or down in the YZ plane adjusting the depth of the probes in relation to the center of the sphere. The maximum depth that measurements are possible is determined by the length of the probe supports. The slides are equipped with precision screw assemblies to make accurate depth measurements convenient. Mounting holes spaced 1" apart the length of the aluminum bar permit probe adjustment in the Y direction. The probes and the sphere were both mounted to the towing carriage as shown in figures 2.1, 2.2, 2.4, and 2.5.

A block diagram of the data collection system employed in the towing tank is shown in figure 2.7. The anemometry system was mounted on the towing carriage and the voltage output was connected to an analog/digital (A/D) input box through data collection cables. A voltage divider composed of two 1/8 watt 1% resistors was used to half the anemometer output voltage so as not to exceed the 10 volt limit of many PC based A/D data collection systems.

The anemometer bridge output voltage was sampled for all probes simultaneously and the average voltage collected. This information was entered into a spreadsheet to develop calibration curves for each probe and wake velocity values. One possible limitation of the one dimensional probes is that they cannot distinguish direction of flow, only magnitude. Thus, to produce useful results the direction of flow must be known. This is not a restriction for the present experiment since the flow in the far wake is unidirectional.

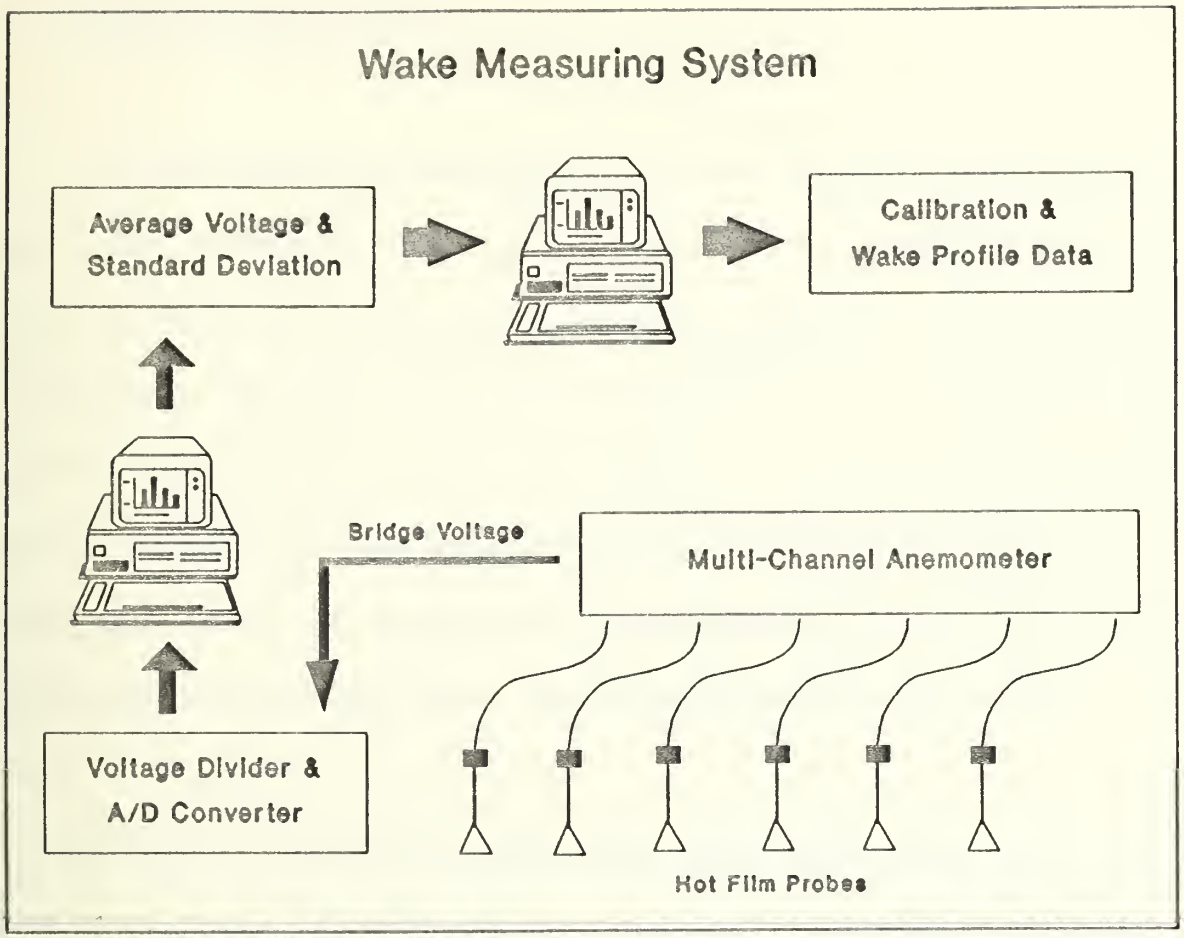

Figure 2.7 Data collection system.

Equipment was setup in the same configuration at both MIT and USNA with some changes to mount the probes and model on the different carriages. The data collection software was also different, but the information collected was the same for both systems with one exception. At USNA, a potentiometer was attached to the carriage drive system and the actual carriage speed was recorded. The MIT carriage does not have this capability, and the average speed was measured over the carriage run. However, the most significant difference was in the way the probes responded to the tank environment of each facility.

2.2 The Data Collection Process

The data collection process consisted of probe calibration and wake velocity measurements. The towing carriage was used to calibrate the hot film probes. The probes were mounted on the carriage with the desired spacing in breadth (Y) and the sphere removed. Output voltages were recorded for a range of speeds centered around the expected wake velocities. When calibration was completed the sphere was mounted and wake measurements recorded for varying values of depth (Z) keeping probe breadth (Y), length (X), and carriage speed constant. The sphere was then removed and the calibration process was repeated with the same range of speeds.

The probes were calibrated in exactly the same environment as they would be taking measurements. This eliminated any constant error sources introduced by the data collection components such as voltage losses in the long data collection cables (100ft), or offsets in the voltage dividers or A/D converter. On the other hand, the accuracy of the calibration was limited by the velocity consistency of the towing carriage.

The anemometer bridge output voltage for each probe was sampled at 100 Hz for 10 to 20 seconds. A sample of the data traces for two probes is shown in figure 2.8. This frequency is above the 20 Hz used at David Taylor Research Center (DTRC)[9], but made measurements possible in the relatively short length of the

---

[9]D. J. Fry and Y. H. Kim "Bow Flow Fields of Surface Ships," Proc. 15th Symposium on Naval Hydrodynamics, (1985).

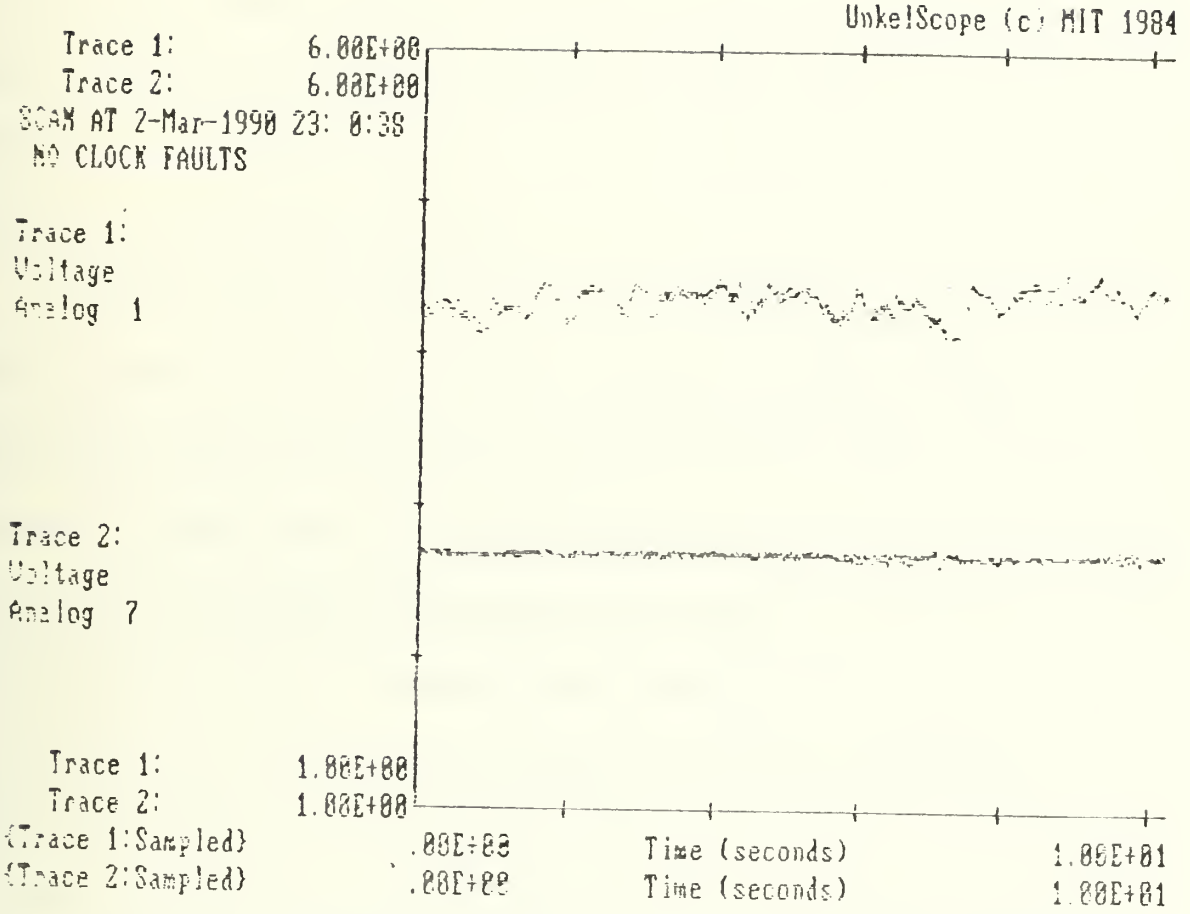

Figure 2.8 Sample data traces for Y = 0 and 1.3 dia.

towing tank. A few comparisons were made from 50 to 200Hz and it was observed that the measurements are insensitive to these higher sampling frequencies.

A dual channel thermistor was placed on the carriage with sensors mounted next to the hot film probes to record any variation in the tank temperature.

The data collected for each constant value of X or Y consisted of time

averaged voltage readings for two calibration runs and a series of wake measurements in the vertical YZ plane. For each averaged voltage reading, tank water temperature and time of data collection were also recorded.

The data collected at USNA consisted of wake measurements in the YZ plane at X = 3, 5, and 7 diameters behind the sphere submerged at 1 dia. The intent here was to investigate how far away from the sphere reliable measurements could be made and to see if the probes could measure a reasonable development of wake profiles as X increased behind the sphere.

The data collected at MIT consisted of more detailed wake measurements in the YZ plane at X = 7 dia. with the sphere submerged one diameter. Wake measurements with the sphere centerline at the water surface and X = 7 dia. were also made. The intent here was to compare wake measurements to the USNA data and to develop more detailed characteristics of the wake at X = 7 diameters. The far field wake at X = 7 dia. was considered a reasonable limit to the measurement of wake profiles for the initial set up of this system and the experimental errors present. Measurements at X = 10 dia. for example would require additional carriage mounting structures and reduce the velocity differences being measured to a very low value and increasing the need for very accurate measurements.

2.3 Developing Calibration Curves

King's law[10] describes the heat transfer from a cylinder of infinite length. This law is the theoretical basis for the development of linear calibration curves used to relate the fluid velocity and bridge output voltage for each probe. It is expressed as shown below.

$$\frac{I^2 R_s}{T_s - T_f} = A_o + B_o \sqrt{Re}$$

I = *Sensor Current,* R_s = *Sensor Resistance,* T_s = *Sensor Temperature*

T_f = *Fluid Temperature,* A_o *and* B_o *are constants and* R_e = *Reynolds number.*

For a hot wire anemometer, Kings law is usually written as

$$E_b^2 = A + BU^n$$

where E_b is the anemometer output voltage, U is the fluid velocity, and A and B are constants. The value of the exponent n varies from 0.45 to 0.5 depending on fluid velocity. This equation does not reflect the sensitivity of the probe to mass flow rate and fluid temperature, but for laboratory measurements at moderate flow velocities

---

[10]L. V. King, "On the convection of heat from small cylinders in a stream of fluid: Determination of the convection constants of small platinum wires with applications to hot-wire anemometry." Phil. Trans. Roy. Soc. (1914) A, 214, 373-432.

it is adequate.[11]

A linear least squares curve fit was passed through the calibration data plotting E_{b2} vs U^n for each probe. A series of values for n were tried and n = 0.5 gave the best curve fit. The constants A and B were also identified.

Probe voltage data were corrected for variations in tank temperature and downward drift with time prior to linear regression. A decrease in tank water temperature will increase the bridge voltage needed to keep the sensor at a constant temperature and be seen as a velocity increase. Conversely, an increase in tank temperature will be seen as a velocity decrease.

The bridge voltage corresponding to a given speed was observed to decrease with time. A possible explanation is that the sensors are insulated by contaminates in the water that adhere to the probes. This would reduce the heat transfer and the required bridge voltage for a given speed. Temperature variations and probe drift are the greatest sources of error in the velocity measurements, but corrections to the data can reduce this error to acceptable levels and yield good results.

The temperature correction applied to the bridge output data is show below.

$$E_{bc} \sim E_b \left[1 - \frac{T_r - T_m}{2(T_s - T_r)}\right]$$

This correction factor was proposed by Bearman[12] and is used to correct for

---

[11]Lomas, p. 62.

[12]P. W. Bearman "Corrections for the effect of ambient temperature drift on hot wire measurements in incompressible flow." DISA Info., (1971) pp. 11, 25-30.

ambient temperature changes. E_{bc} is the corrected bridge voltage, T_r is an arbitrary reference temperature, T_s is the sensor temperature, and T_m is the tank temperature measured by the dual channel thermistor mounted on the carriage. This correction worked well when the ambient change was gradual over a long period of time. If longitudinal or vertical temperature gradients of 2°C or more were present in the tank this correction factor did not produce consistent results. This is because the ambient temperature correction does not compensate for temperature changes during a data run.

At USNA there were no detectable temperature gradients in the tank and only small variations occurred over several days. This is due to the position of the tank in the middle of a large well air conditioned room. At MIT longitudinal and vertical temperature gradients were observed greater than 2°C. To correct for this the water was stirred up using an electric outboard trolling motor prior to collecting data. The position of the MIT tank against the wall of the building, a small heating and air conditioning system and large temperature differences outside and inside all contributed to the strong temperature gradients.

When using hot film probes in water the temperature of the probe is limited by the boiling point. Thus, the practical limit of sensor temperature is around 70°C and the maximum difference between the sensor and the environment is about 50°C. Under these conditions a 2°C difference in tank temperature will produce a 2% change in bridge voltage. From King's law, velocity increases as the fourth power of bridge voltage and small temperature variations will quickly introduce large errors in the velocity measurements. When measuring far field wake velocities where the

maximum velocity deficit is a small percentage of the free stream, an 8% velocity error is significant.

When using hot wire probes in air the temperature difference between the sensor and probe is on the order of 200°C and the effect of small temperature variations is reduced.

An alternative temperature correction method "requires the construction of a series of calibration curves over the range of the ambient temperature variations expected. If ambient temperature is monitored separately, each output voltage reading can be converted to velocity by interpolating the calibration curves."[13] This method is impractical for use in a towing tank due to the difficulty of controlling water temperature, but it was used to correct for the observed drifting of the probes.

As mentioned above, calibration data were collected before and after wake measurements. The second calibration run produced a curve similar in slope to the first but offset with a lower intercept. This drifting of the probes was assumed to be a function of time and individual probe characteristics. Thus, the temperature corrected wake measurement voltages were converted to velocities by interpolating the calibration curves as a function of time.

The interpolation scheme used is described below. Each calibration speed was repeated before and after wake measurements at equally spaced time intervals. A "drift factor" was calculated for each speed in volts/time. These drift factors were averaged over the calibration speed range to produce an average drift correction for

---

[13]Lomas, p. 77.

each probe. This drift factor was used to correct each calibration reading back to a common time. Thus, the calibration data were plotted as if it were collected simultaneously. After this correction was applied, a single calibration curve for each probe was fit to the data using King's law.

A summary of the results from linear regression of the calibration data are shown in appendix A. A sample of one calibration plot is included in figure 2.9; this

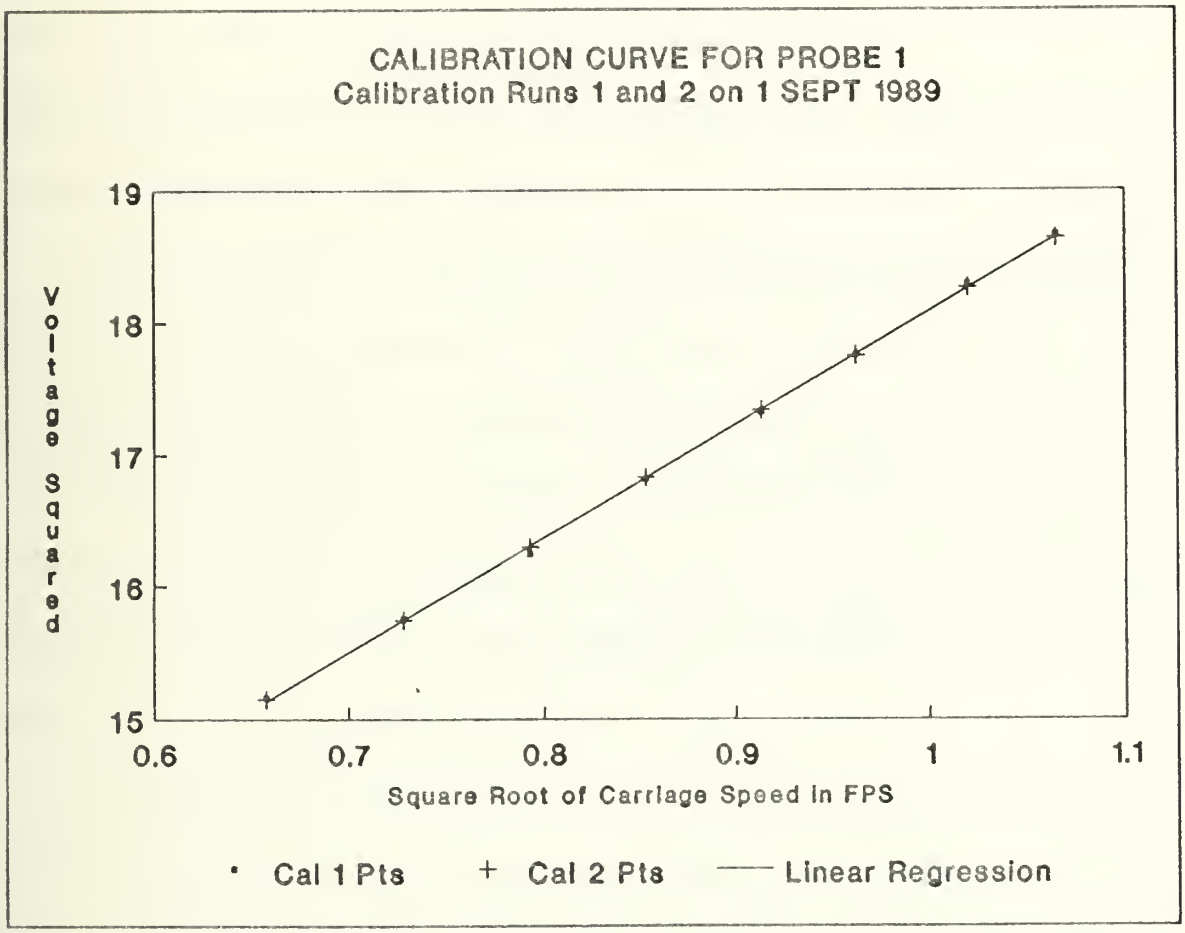

Figure 2.9 Sample calibration plot.

plot corresponds to the regression results for probe one shown on table A.2 in appendix A. The fit of calibration data to King's law is very good. This agreement with established theory after the temperature and drift corrections are applied

strongly supports the feasibility of this measuring system. The King's law curve fits had less error when both sets of calibration data were used suggesting that an ensemble average of many calibration runs would converge to the theoretical result.

The magnitude of the average drift correction was generally larger than the temperature corrections and is felt to be the primary source of error in the experiment. There is no sound theoretical basis for the cause of the drift. At USNA the probes were left on and in the water for a week in hopes that the probes would come to some kind of equilibrium with their environment. It was observed that the amount of drift decreased but did not stop completely. The sensitivity of the probes to velocity changes also seemed to decrease when left in the water for several days.

The probes could be cleaned to restore sensitivity, but would not eliminate the drift as new clean probes seemed to drift the most. Several hours were needed to collect wake measurements and calibration data due to the 8-14 minute time delay between carriage runs needed to store the probe data and allow the tank to return to equilibrium. The many carriage runs required to calibrate and measure the wake prevented rapid collection of data, and drift, even though slow over time was always a major source of measurement error.

The water in the towing tanks at USNA and MIT was city tap water and no special treatment was added to the tanks prior to data collection. No visible buildup of contaminates on the probes was noted. The drift was more steady and uniform at USNA when the probes were left in the water for long periods of time. At MIT the probes were not left on due to limited tank availability and adjustments of the probes in the Y dimension that required removal and reinstallation. The drift was

more erratic and the calibration plots had more scatter in the data, but curve fits still yielded good results.

When additional measurements are conducted in the future some investigations should be made into chemical or other water treatment methods that could possibly eliminate insulation of the probes and the resulting drift of calibration readings and wake measurements.

2.4 Collection and Conversion of Wake Measurement Data

Wake measurements were collected in the positions described below and the measured bridge voltages converted to wake velocities using the calibration data in Appendix A. A summary of all wake velocity measurements used to plot the wake profiles are included in Appendix B. The procedure used to convert the bridge voltages to wake measurements is also described below.

At USNA, five probes were mounted on the probe rack at Y = $\pm$0.81, $\pm$0.58, and 0 diameters. For values of X = 3, 5 and 7 dia., multiple data runs at constant speed were made at values of Z = -0.93, -0.7, $\pm$0.47, $\pm$0.23, and 0 dia.

At MIT, X was held at 7 dia and two arrangements of Y values were used. The first was symmetric with 7 probes mounted at Y = $\pm$1.3, $\pm$0.81, $\pm$0.35 and 0 dia. The range of Y was increased over that used at USNA to ensure the limits of the wake were reached. The second was concentrated on one side using 6 probes with Y = -1.3, -0.93, -0.58, $\pm$0.24 and 0 dia. This arrangement was selected to further refine the transition from the maximum wake deficit to the free stream. Values of

Z = ±0.81, ±0.58, ±0.35, ±0.12, and 0 dia. were used for both arrangements. All of the above measurements were taken with the center of the sphere submerged one diameter.

Additionally, the two ranges of Y values described above were used to collect wake data with the center of the sphere at the surface of the water and X = 7 dia. Values of Z = -0.81, -0.58, -0.35, and -0.12 dia. were used for both arrangements. The results of these measurements are summarized in chapter 3.

The same sampling frequencies used for calibration runs were also used for wake measurements. For each measurement run the tank temperature and time of the run was recorded. This information was used to apply temperature and drift corrections to the wake measurement data. The temperature correction was applied in the same manner as for the calibration curves. The average drift factor was used to correct the wake measurement data to the common reference time of the calibration curve. Then, the calibration curve was used to convert the wake measurement voltages to wake velocities.

This procedure produced many wake velocity measurements greater than the free stream value. While wake velocities greater than the free stream are possible close behind the sphere, this is not possible at the values of X = 3 to 7 dia. and is therefore a measurement error. This error is most likely the caused by nonlinear drift of the probes.

The interpolation scheme assumes that the probe drift is a constant linear function of time. If the drift was a nonlinear function of time or influenced by other variables such as probe velocity or water temperature than the average drift

corrections could deviate from the actual drift at the time of wake measurements.

To correct what is perceived to be an obvious error in the data, two additional drift corrections were made. The first was to assume that the data run at the lowest value of Z (-0.81 or -0.93 dia.) was in the free stream and a constant value was subtracted or added from all the velocity measurements of each corresponding probe to impose this assumption on the wake measurement data. The second was to decrease the average drift factor to prevent any other velocity measurements from reading above the free stream.

A sample of the calibration and wake conversion calculations are included in Appendix C.

Chapter 3: SUMMARY OF RESULTS

3.1 Surface Fit of Wake Data

Tables 3.2 and 3.3 are a summary of where wake measurements were taken. All dimensions listed are in diameters of the sphere (1 dia. = 8.6 in.). For each Y value listed measurements were taken at all Z values and vice versa. The figures listed at the bottom of the table are the plots made from the data taken at these positions. The names "Wake One, Wake Two, etc." are arbitrary titles.

All the plots shown are representations of a polynomial surface using 25 coefficients that was passed through the wake measurement data for each value of X. The surfaces represented should only be used for ranges of Y and Z for which data was taken. Any extrapolation outside this range will quickly lead to large errors. The equation of the surfaces is shown below. The summary of errors

$$Velocity = f(Y,Z) = \sum_{j=0}^{4} \sum_{i=0}^{4} a_{ij} Y^i Z^j (8.6)^{(i+j)}$$

between the surface fit and actual data is shown in table 3.1 and the coefficients a_{ij}

Table 3.1 Summary of Surface Fit Errors

Error in %	Wake One	Wake Two	Wake Three	Wake Four	Wake Five
Max	$2.766e^{-2}$	$1.653e^{-2}$	$1.575e^{-2}$	0.1432	$4.234e^{-2}$
Ave	$6.734e^{-3}$	$3.318e^{-3}$	$4.817e^{-3}$	$2.767e^{-2}$	$9.260e^{-3}$
Var	$6.585e^{-5}$	$1.426e^{-5}$	$1.643e^{-5}$	$1.095e^{-3}$	$1.162e^{-4}$

are listed in table 3.4. Y and Z are coordinates in the YZ plane referenced to the center of the sphere in diameters. The term $(8.6)^{(i+j)}$ is a conversion factor. The function f(YZ) is equal to the relative velocity deficit compared to the free stream at the position YZ. A listing of the fortran program written by LCDR Frank Camelio that was used to create these surfaces is include in Appendix D.

Table 3.2 Summary of Wake Measurements Taken at USNA

(all units in sphere diameters, 1 dia = 8.6in.)

Sphere submerged to 1 dia. Below Free Surface

Wake One		Wake Two		Wake Three	
X = 3		X = 5		X = 7	
Y	Z	Y	Z	Y	Z
± 0.81	-0.93	± 0.81	-0.93	± 0.81	-0.93
± 0.35	-.70	± 0.35	-0.70	± 0.35	± 0.70
0	± 0.47	0	± 0.47	0	± 0.47
	± 0.23		± 0.23		± 0.23
	0		0		0
Plotted in fig. 3.1 - 3.4.		Plotted in fig. 3.5 - 3.8.		Plotted in fig. 3.9 - 3.12.	

Table 3.3 Summary of Wake Measurements Taken at MIT (All dimensions in sphere diameters, 1 dia. = 8.6 in.)			
Wake Four (X = 7)		Wake Five (X = 7)	
(Center of Sphere Submerged 1 dia.)		(Center of sphere on surface)	
Y	Z	Y	Z
± 1.28	± 0.81	± 1.28	-0.81
-0.93	± 0.58	-0.93	-0.58
± 0.81	± 0.35	± 0.81	-0.35
-0.58	± 0.12	-0.58	-0.12
± 0.35	.0	± 0.35	
± 0.23		± 0.23	
0		0	
Plotted in fig. 3.13-3.17.		Plotted in fig. 3.17 - 3.20.	

Table 3.4 Polynomial Coefficients for Wake Surfaces (A_{ij})					
ij	Wake One	Wake Two	Wake Three	Wake Four	Wake Five
00	0.9076	0.9388	0.8876	0.8301	0.9120
10	$2.119e^{-3}$	$7.907e^{-3}$	$3.807e^{-3}$	$-1.185e^{-2}$	$8.469e^{-3}$
20	$7.922e^{-3}$	$2.028e^{-3}$	$1.264e^{-2}$	$1.854e^{-2}$	$1.471e^{-3}$
30	$-8.154e^{-7}$	$-7.311e^{-5}$	$-1.234e^{-4}$	$-2.863e^{-3}$	$-6.554e^{-5}$
40	$-1.326e^{-4}$	$-3.289e^{-5}$	$-2.237e^{-4}$	$1.261e^{-4}$	$-1.052e^{-5}$
01	$6.339e^{-3}$	$-1.271e^{-2}$	$-2.093e^{-2}$	$-1.498e^{-2}$	$-1.387e^{-2}$
11	$3.019e^{-3}$	$7.338e^{-4}$	$2.687e^{-3}$	$-1.242e^{-2}$	$4.819e^{-4}$
21	$-3.486e^{-3}$	$3.345e^{-4}$	$1.963e^{-3}$	$1.865e^{-3}$	$1.762e^{-3}$
31	$-5.597e^{-5}$	$-5.348e^{-6}$	$-5.833e^{-5}$	$6.494e^{-5}$	$2.775e^{-5}$
41	$6.724e^{-5}$	$-4.567e^{-6}$	$-3.443e^{-5}$	$-1.117e^{-5}$	$-1.868e^{-5}$
02	$2.164e^{-3}$	$6.049e^{-4}$	$8.778e^{-4}$	$1.524e^{-3}$	7.21
12	$7.132e^{-4}$	$-2.026e^{-4}$	$3.208e^{-4}$	$2.614e^{-3}$	-9.21
22	$-5.962e^{-4}$	$-8.719e^{-5}$	$-3.041e^{-4}$	-2.589^{-3}	6.440
32	$-1.653e^{-5}$	$2.305e^{-6}$	$-4.115e^{-6}$	$4.620e^{-4}$	$2.313e^{-5}$
42	$1.156e^{-5}$	$1.776e^{-6}$	$5.455e^{-6}$	$-2.270e^{-5}$	$-8.210e^{-6}$
03	$-1.238e^{-3}$	$1.375e^{-4}$	$2.324e^{-4}$	$-5.538e^{-5}$	$3.026e^{-3}$
13	$1.332e^{-5}$	$2.766e^{-5}$	$-7.817e^{-5}$	$2.807e^{-4}$	$-2.483e^{-4}$
23	$2.063e^{-4}$	$-1.647e^{-5}$	$-5.327e^{-5}$	$-8.193e^{-5}$	$6.725e^{-5}$
33	$-8.054e^{-7}$	$-5.585e^{-7}$	$1.657e^{-6}$	$8.915e^{-6}$	$4.720e^{-6}$
43	$-3.593e^{-6}$	$3.273e^{-7}$	$9.322e^{-7}$	$-3.402e^{-7}$	$-1.219e^{-6}$
04	$-1.549e^{-4}$	$-2.461e^{-6}$	$2.052e^{-6}$	$-1.376e^{-5}$	$2.812e^{-4}$
14	$-4.196e^{-6}$	$6.210e^{-6}$	$-1.060e^{-5}$	$-4.222e^{-5}$	$-1.879e^{-5}$
24	$2.658e^{-5}$	$-5.262e^{-7}$	$-1.184e^{-6}$	$3.870e^{-5}$	$9.871e^{-7}$
34	$5.025e^{-8}$	$-9.997e^{-8}$	$1.902e^{-7}$	$-6.821e^{-6}$	$3.104e^{-7}$
44	$-4.700e^{-7}$	$1.211e^{-8}$	$1.906e^{-8}$	$3.334e^{-7}$	$-5.666e^{-8}$

3.2 Graphs of Wake Measurements

The wake profile surfaces are plotted on the following pages. Each wake surface is shown in four separate graphs. These different plots give the reader several views of the same surface so details not apparent in one view may be clear in another.

The first plot of each wake is a three dimensional plot of the polynomial surface. The vertical axis is the relative velocity deficit of the wake. A value of 1.0 represents the free stream and a lower value, the velocity reduction in the wake. For example, a relative velocity of 0.80 means that the velocity measured is 80% of the free stream velocity. The horizontal axis of depth and breadth represent the plane in which the velocity measurements were made. The curved lines used to represent the surface are values of constant breadth in one direction and constant depth in the opposite direction. The wake appears as a valley that rises up to a plateau as depth and breadth increase.

The second graph is the same as the first except that the lines used to represent the surface are values of constant relative velocity.

The third plot shown for each wake is a two dimensional contour plot of the polynomial surface. The axis are breadth and breadth. The lines shown are values of constant velocity. These lines are the same as those in the second plot mentioned above except that it is presented in two dimensions instead of three. This plot is the best from which to estimate the velocity of the wake at a particular point.

The last graph of each wake is a two dimensional plot of breadth vs relative velocity at four values of constant depth. One curve shows the shape of the surface

at the largest value of depth for which data was collected. Another shows the shape at the center of the sphere (depth = 0). The remaining two lines are equal distances above and below the center of the sphere at values equal to half the difference between the center of the sphere and the largest value of depth. If more than four lines are plotted the graph becomes cluttered and hard to understand.

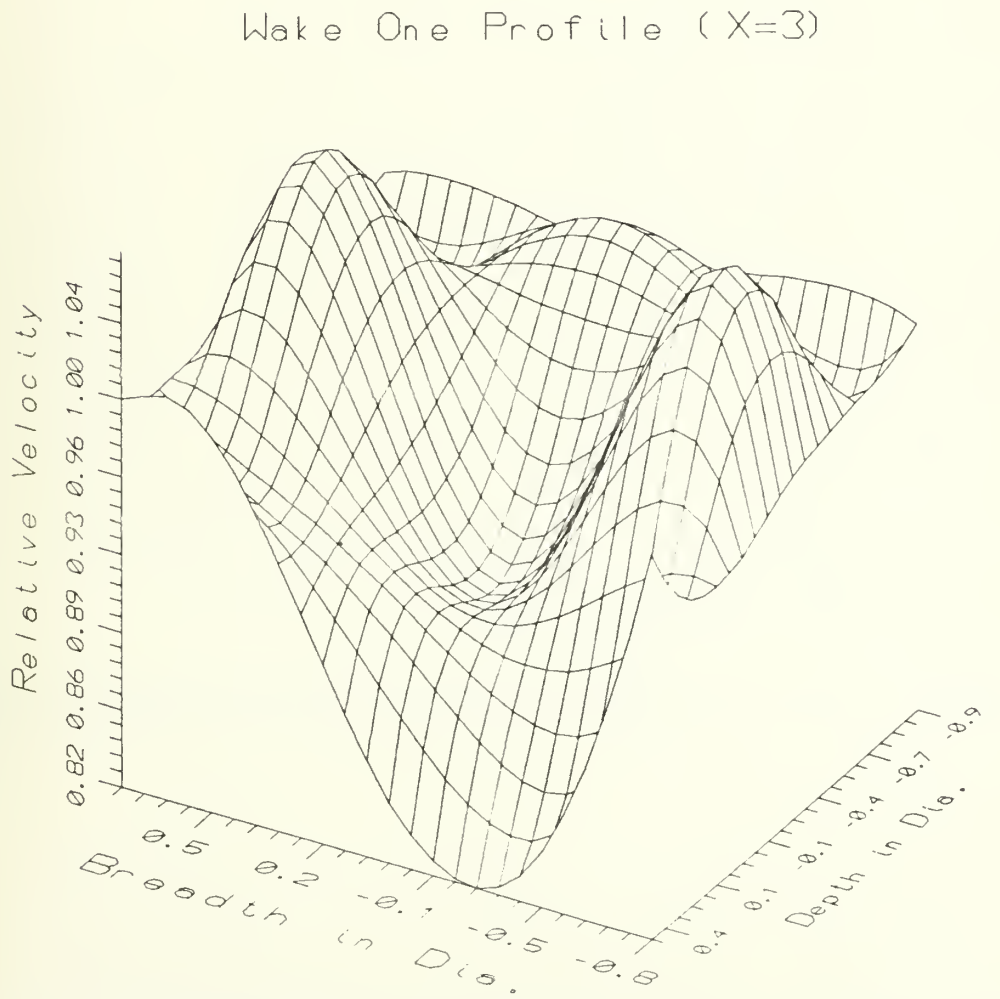

Figure 3.1 Wake one profile.

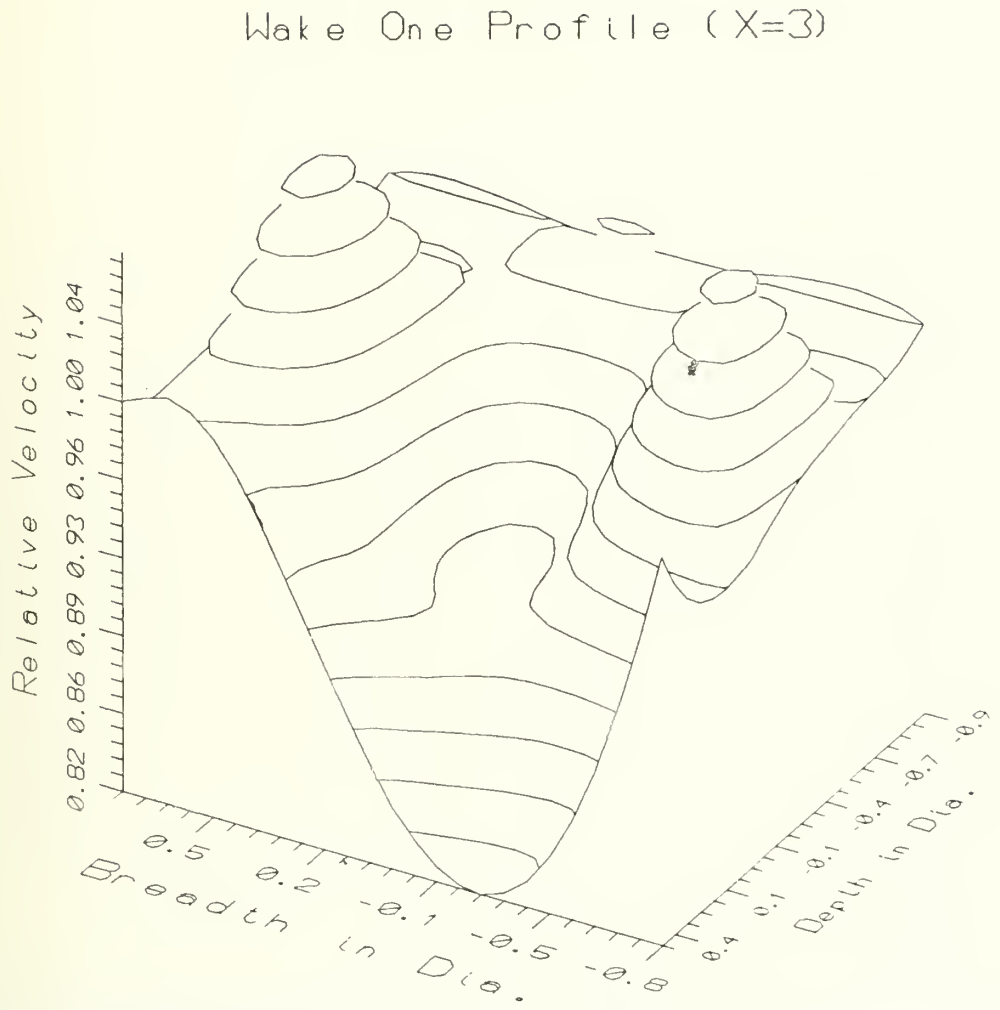

Figure 3.2 Wake one contours of constant velocity.

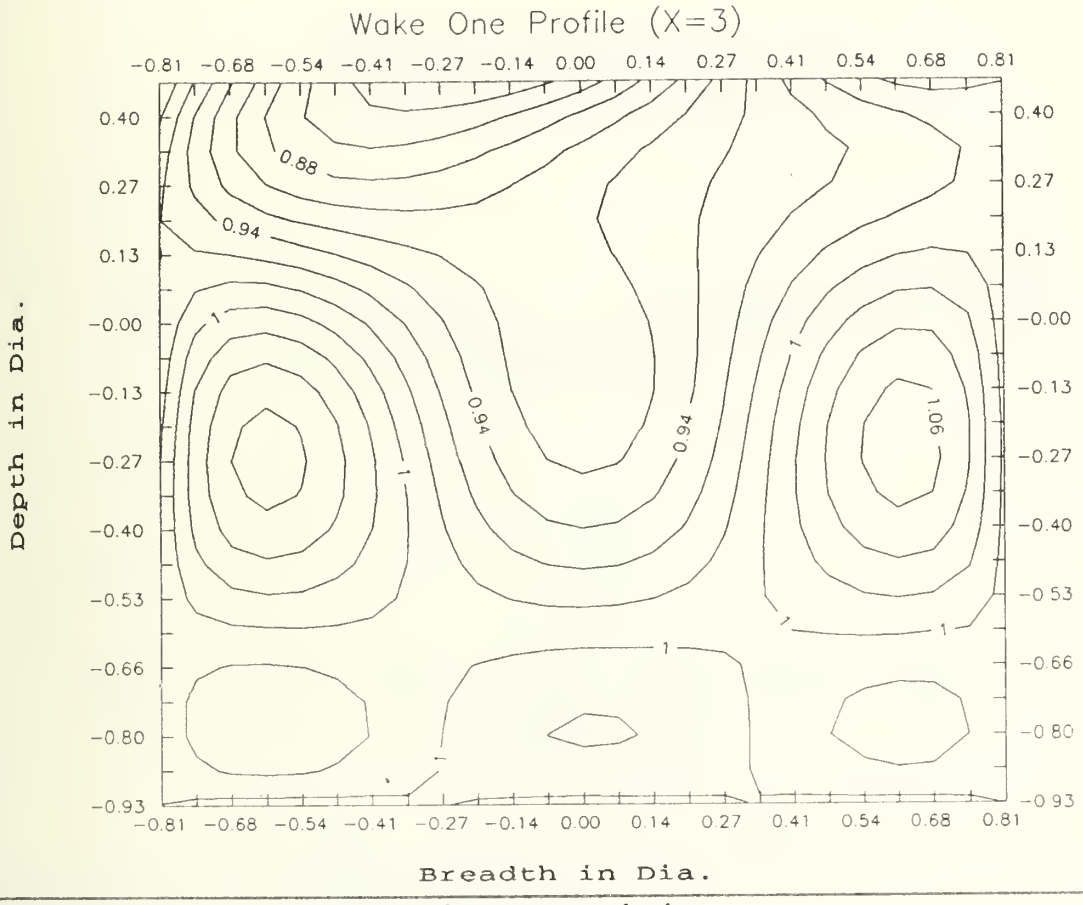

Figure 3.3 Wake one contours of constant velocity.

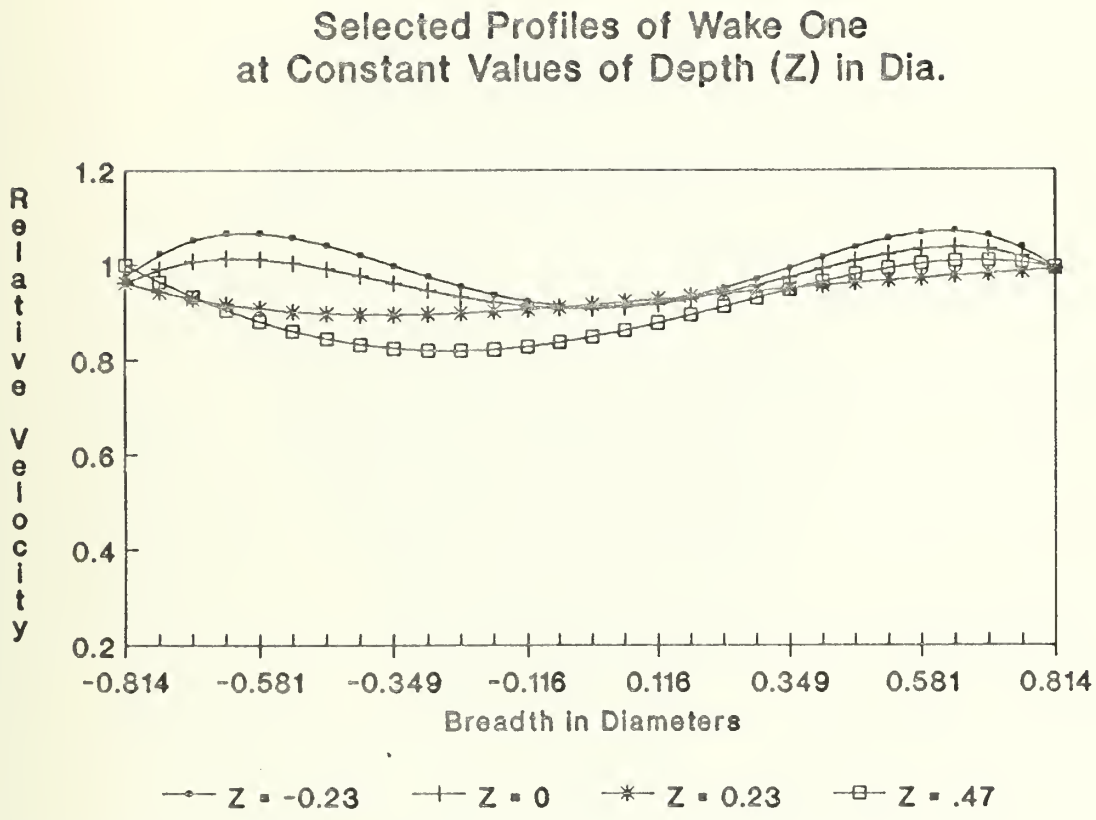

Figure 3.4 Selected profiles of wake one.

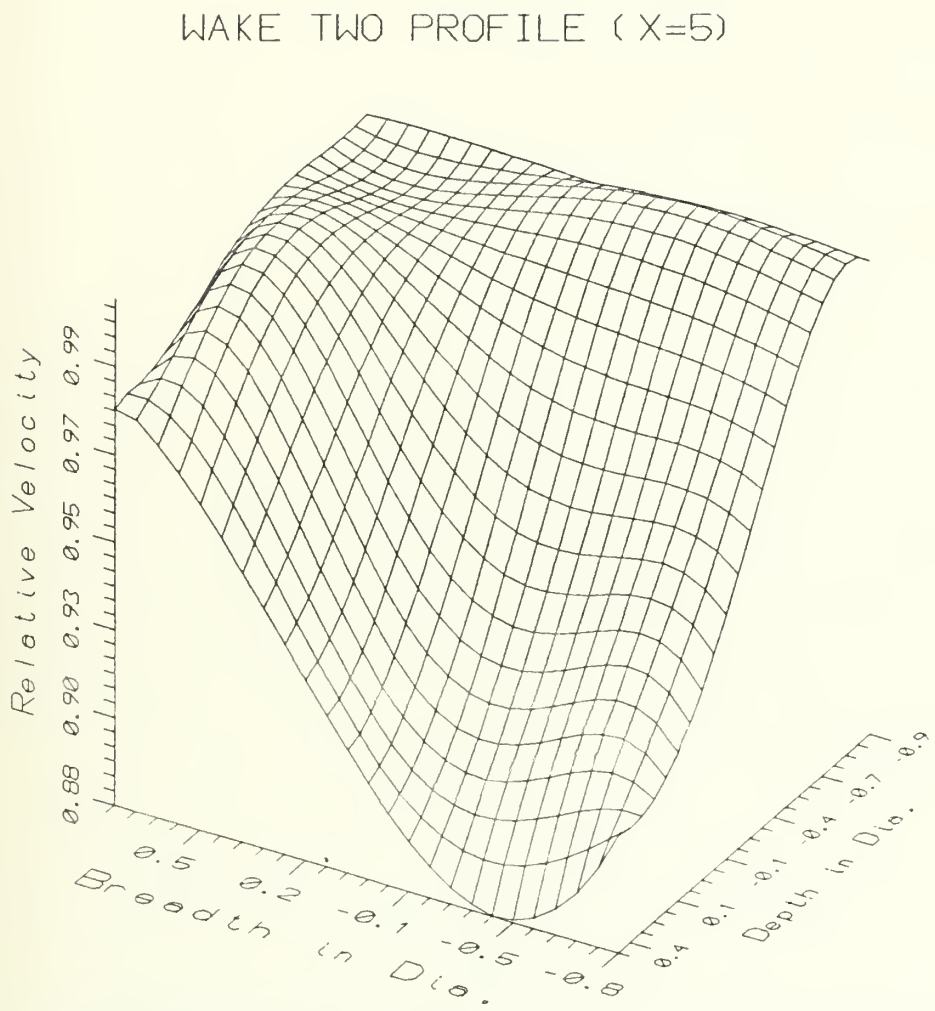

Figure 3.5 Wake Two Profile.

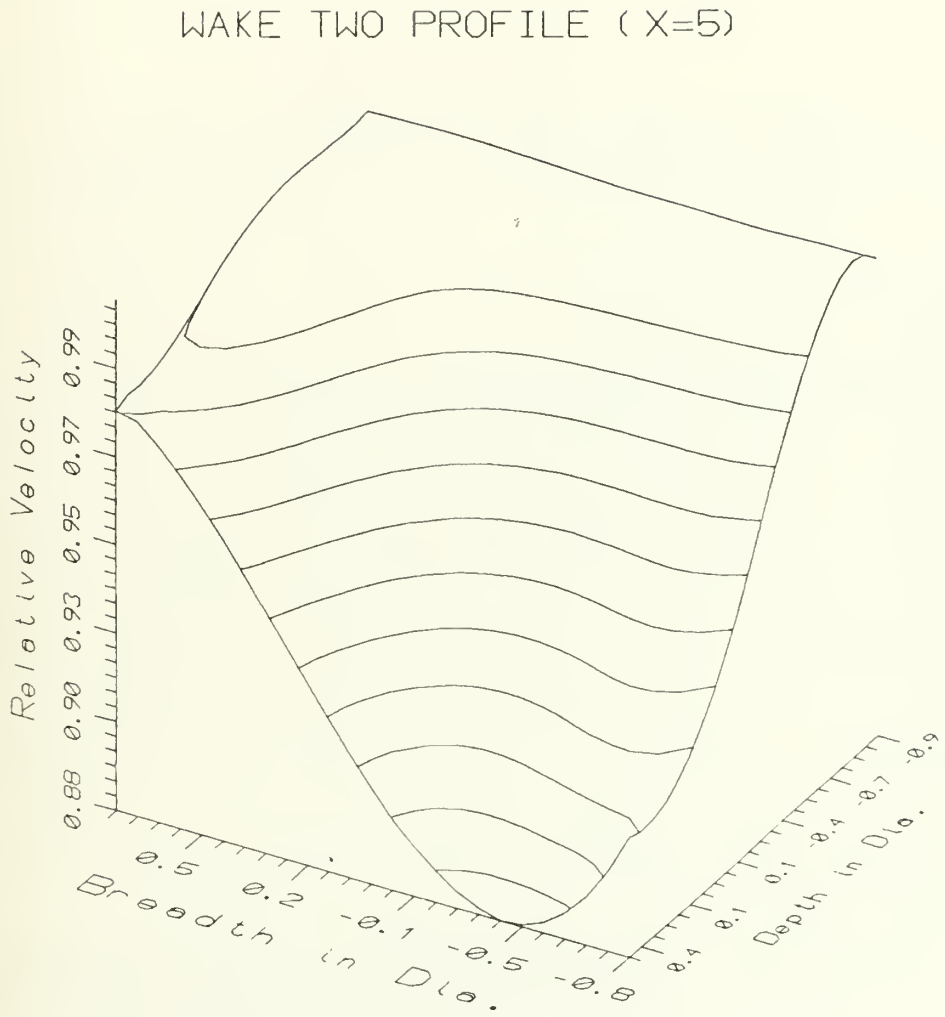

Figure 3.6 Wake two profiles of constant velocity.

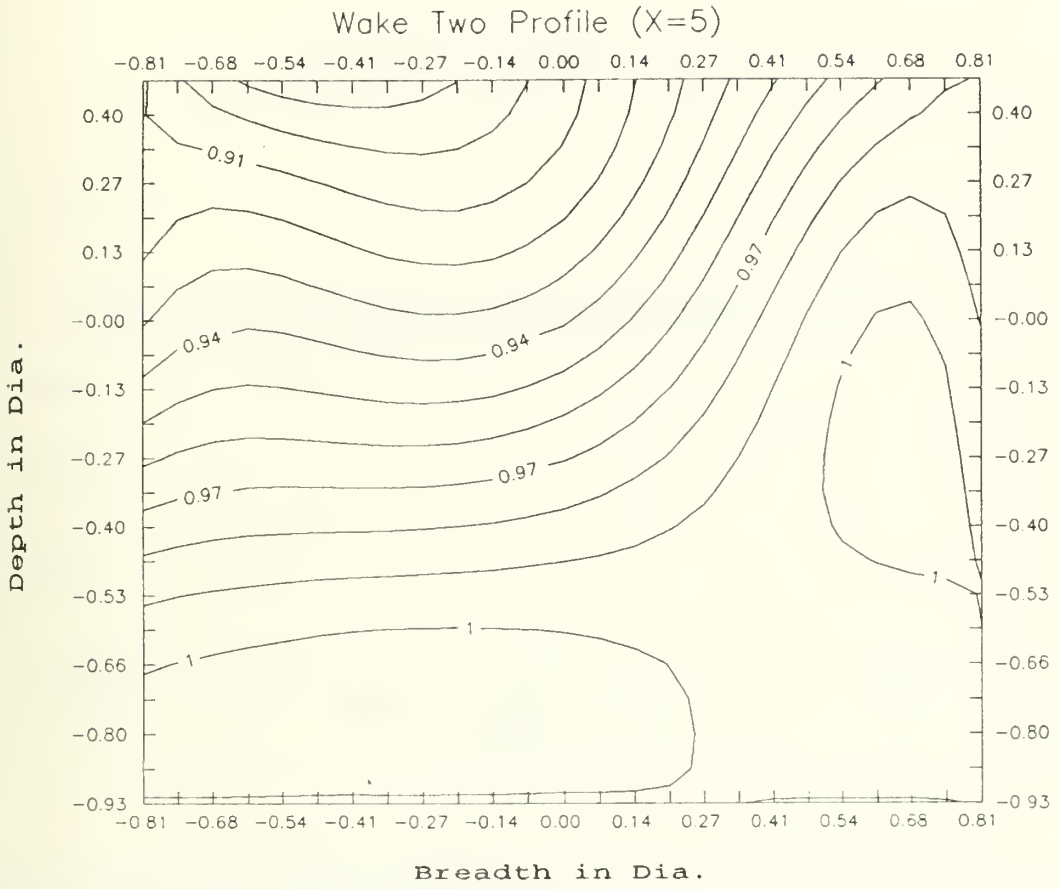

Figure 3.7 Wake two contours of constant velocity.

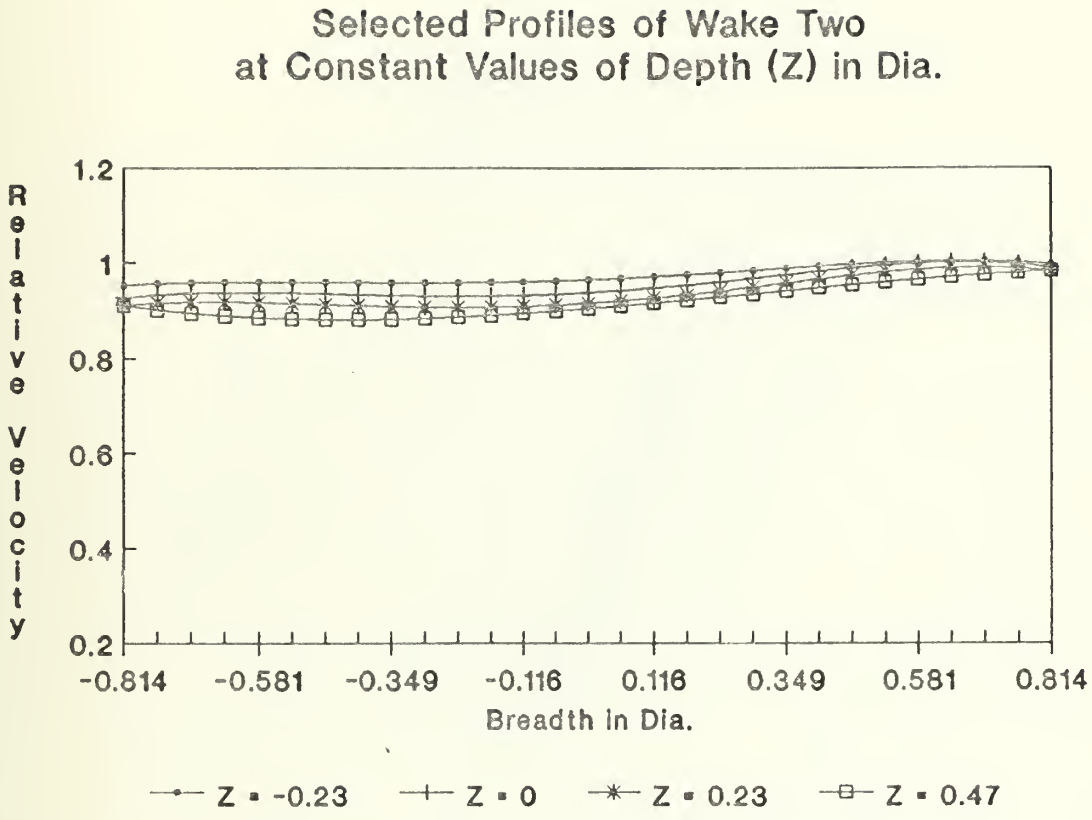

Figure 3.8 Selected profiles of wake two.

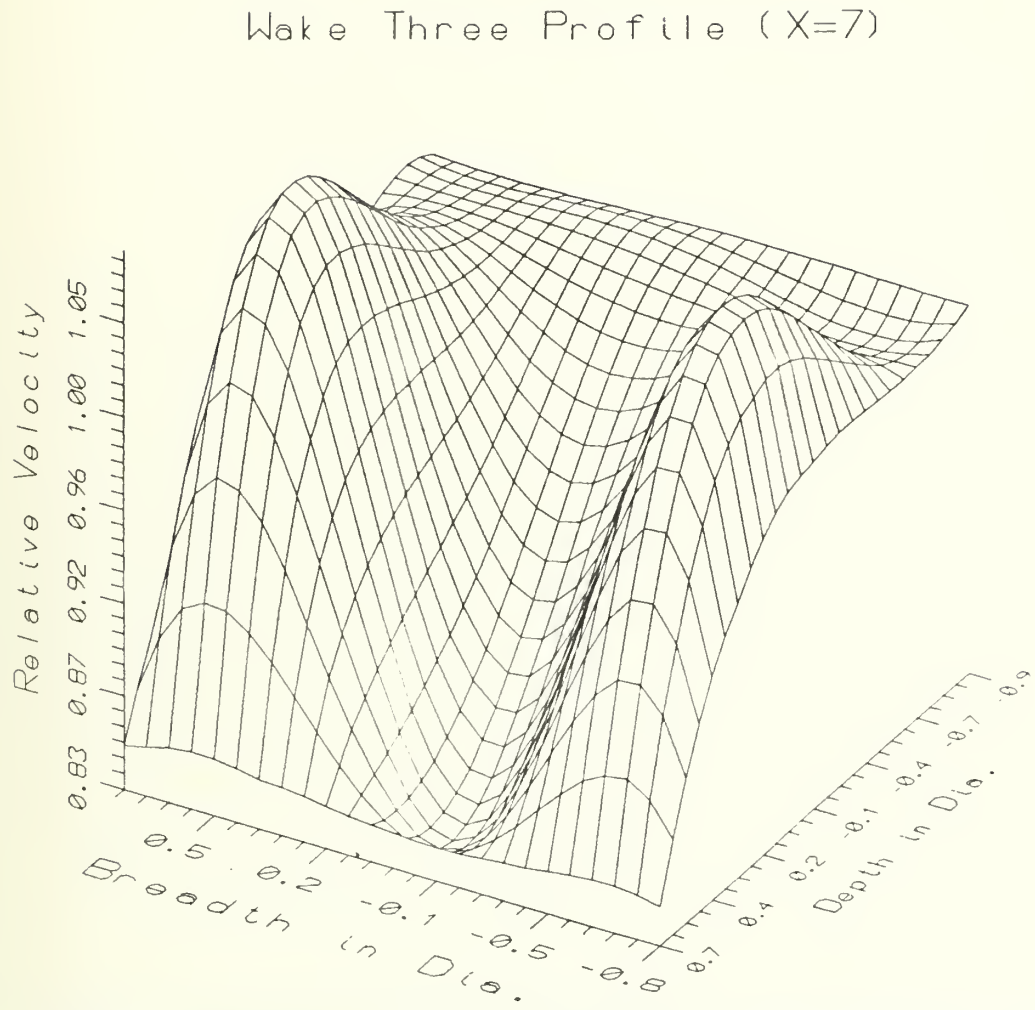

Figure 3.9 Wake Three Profile.

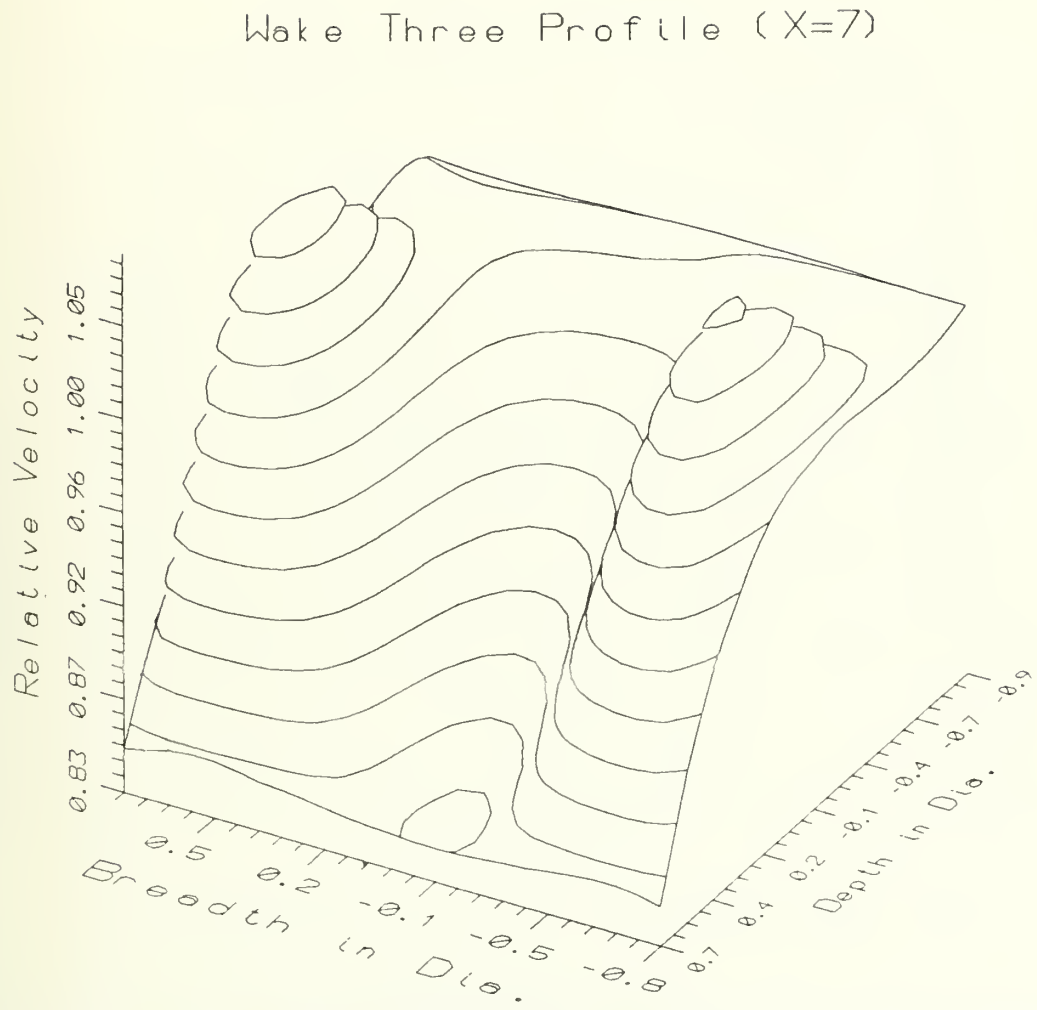

Figure 3.10 Wake three profiles of constant velocity.

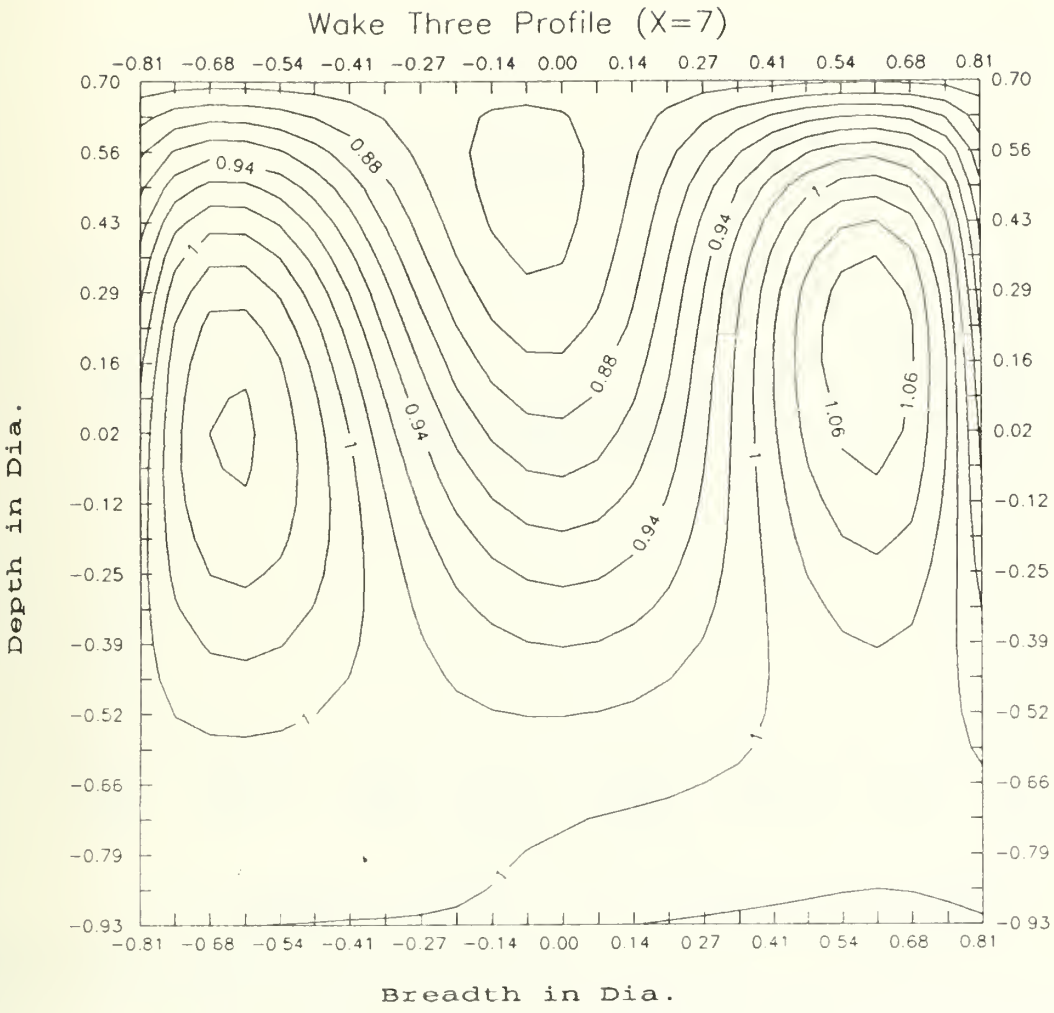

Figure 3.11 Wake three contours of constant velocity.

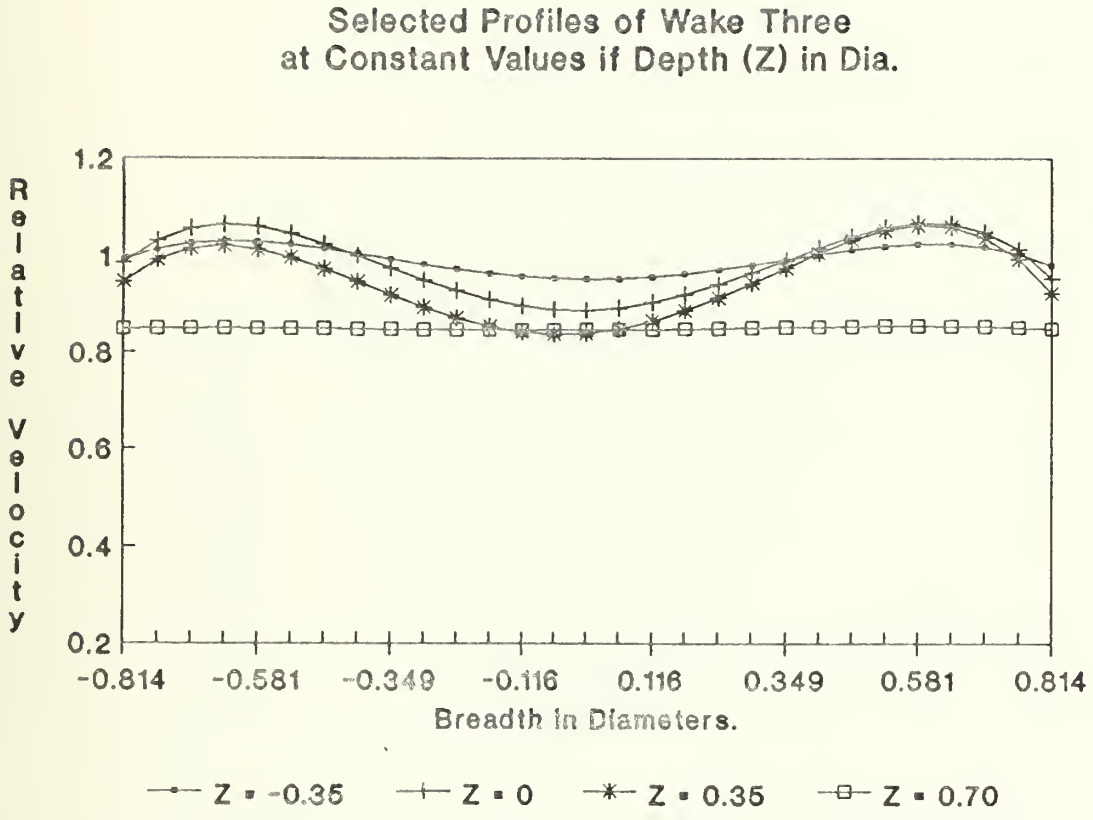

Figure 3.13 Selected profiles of wake three.

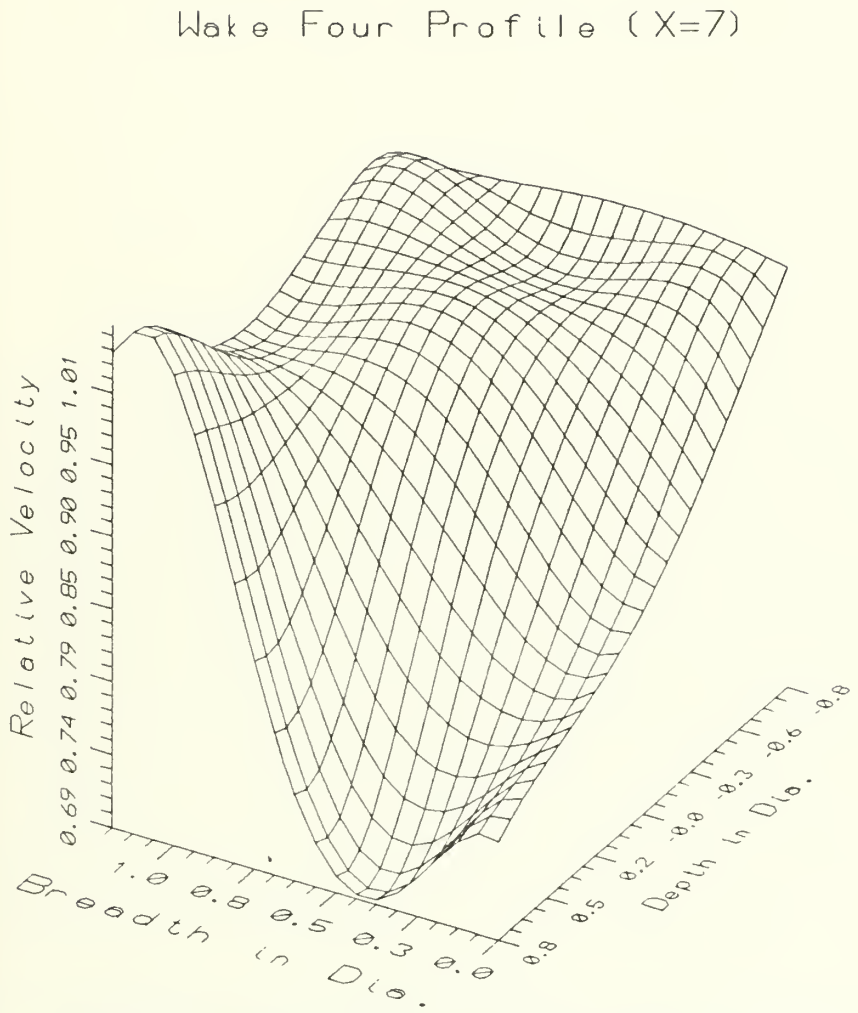

Figure 3.13 Wake four profile.

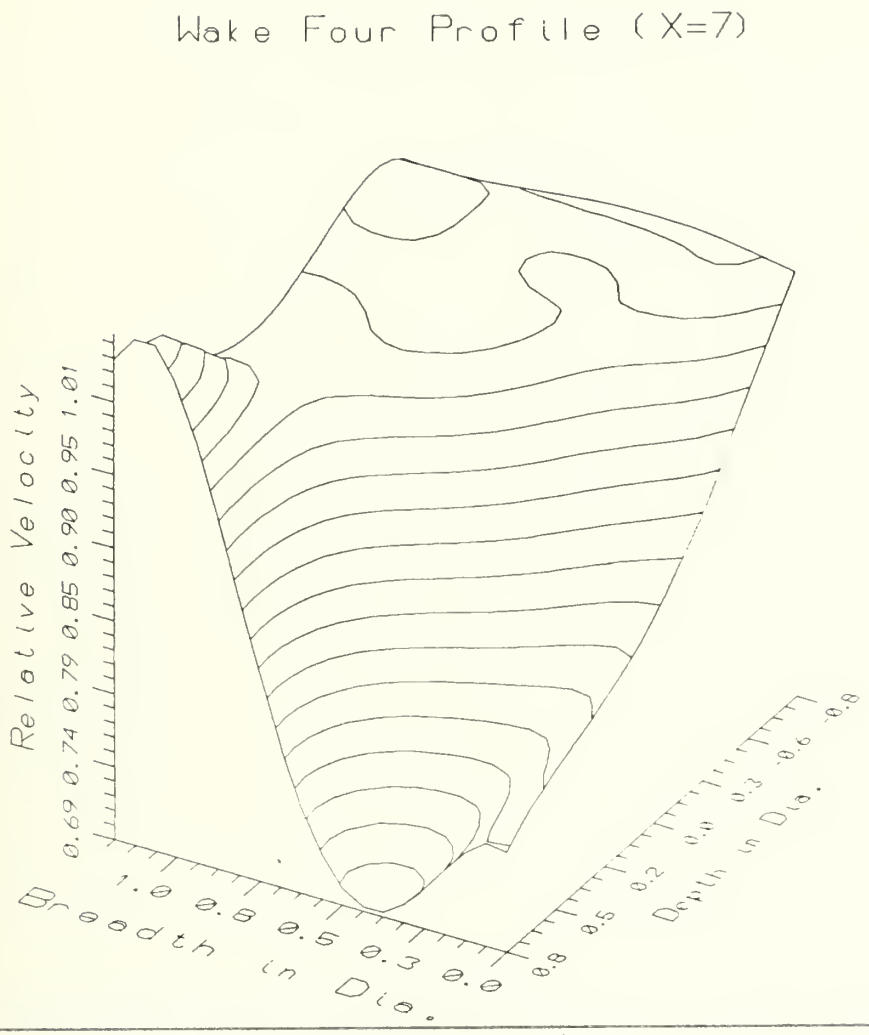

Figure 3.14 Wake four profiles of constant velocity.

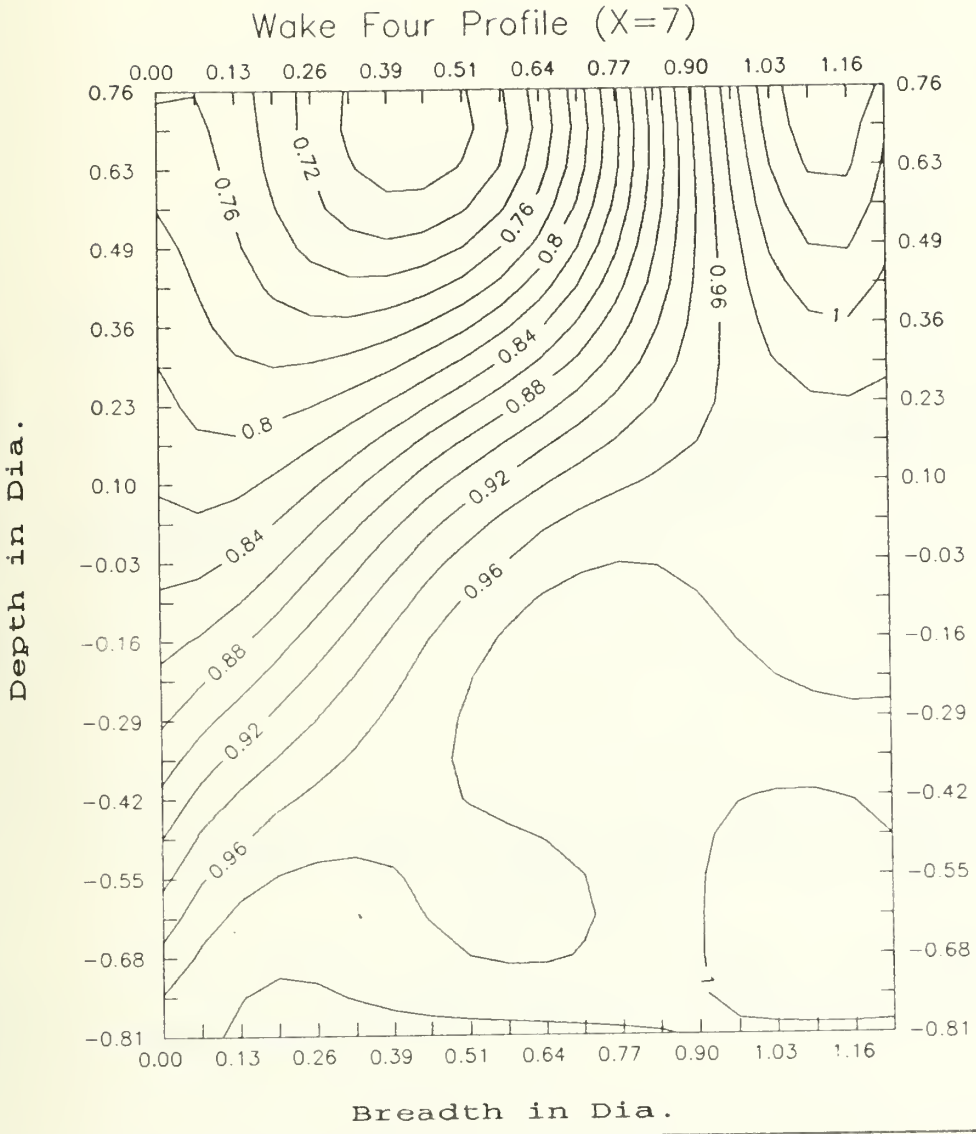

Figure 3.15 Wake four contours of constant velocity.

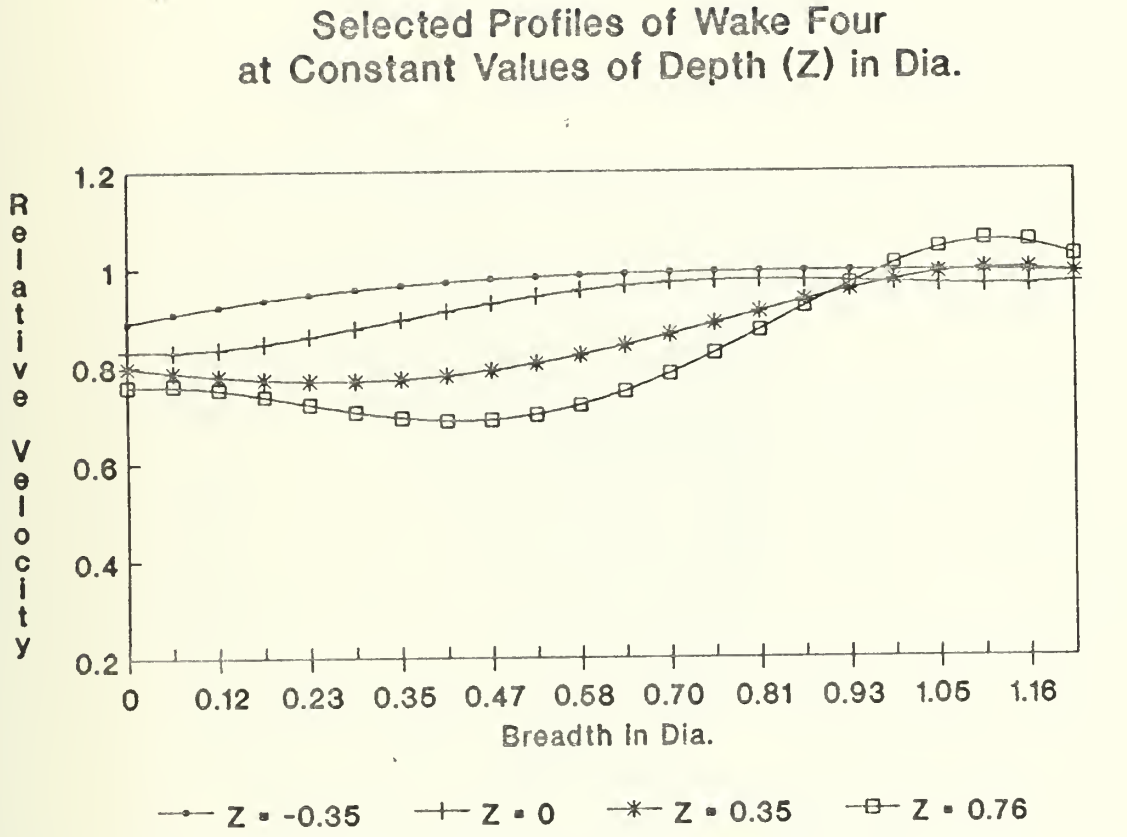

Figure 3.16 Selected profiles of wake four.

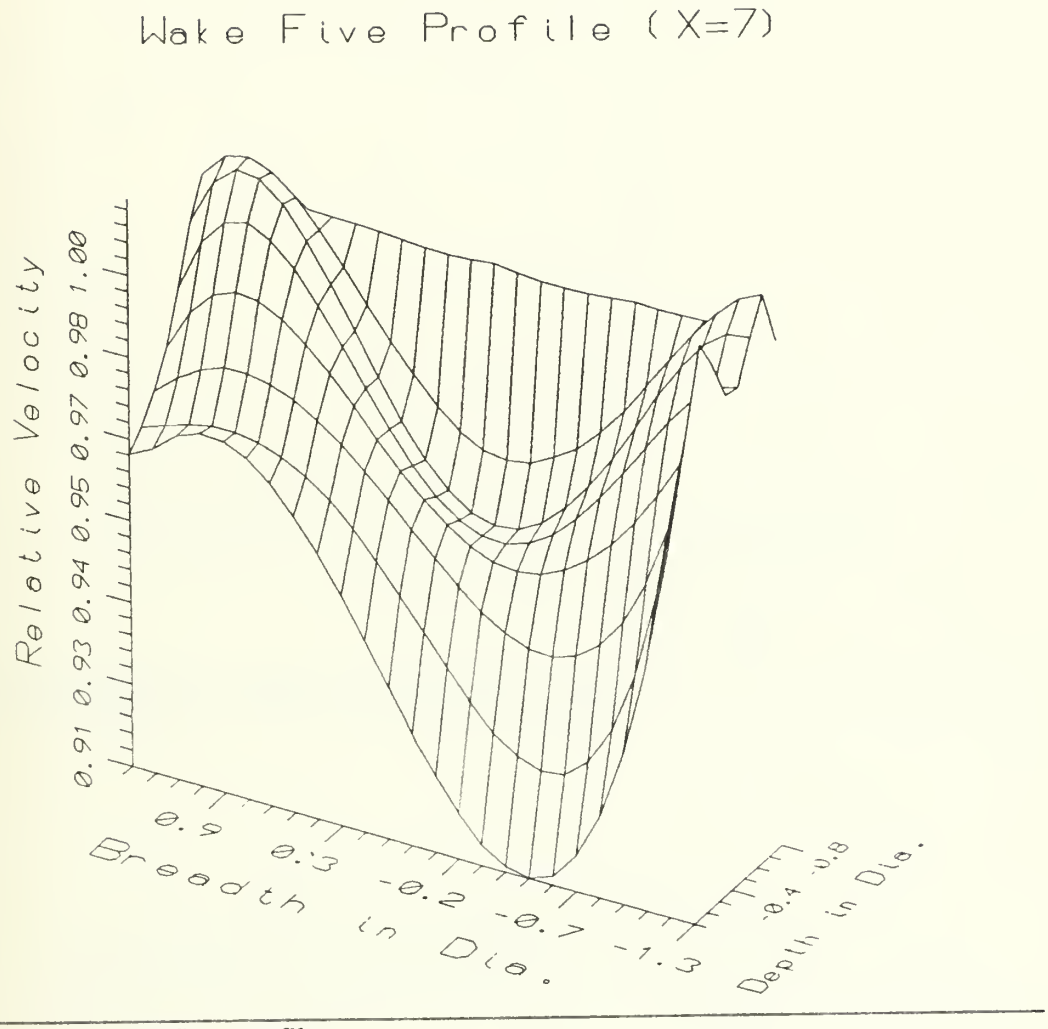

Figure 3.17 Wake five profile.

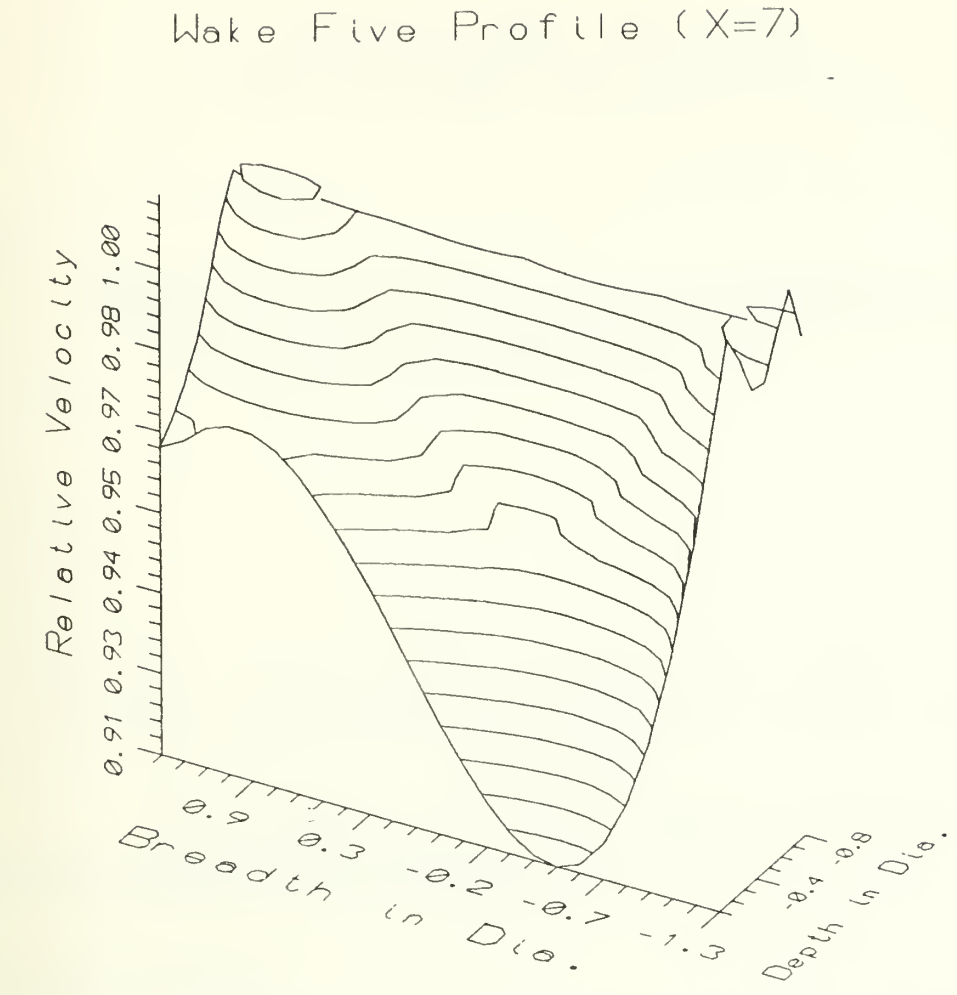

Figure 3.18 Wake five profiles of constant velocity.

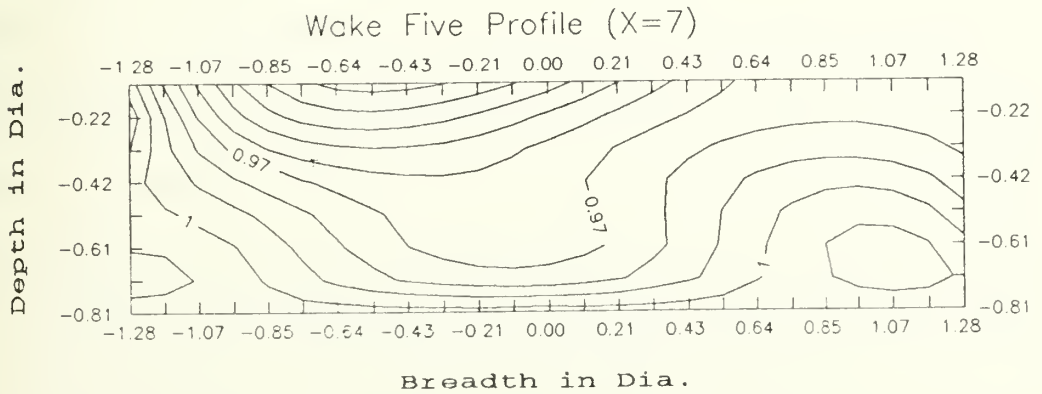

Figure 3.19 Wake five contours of constant velocity.

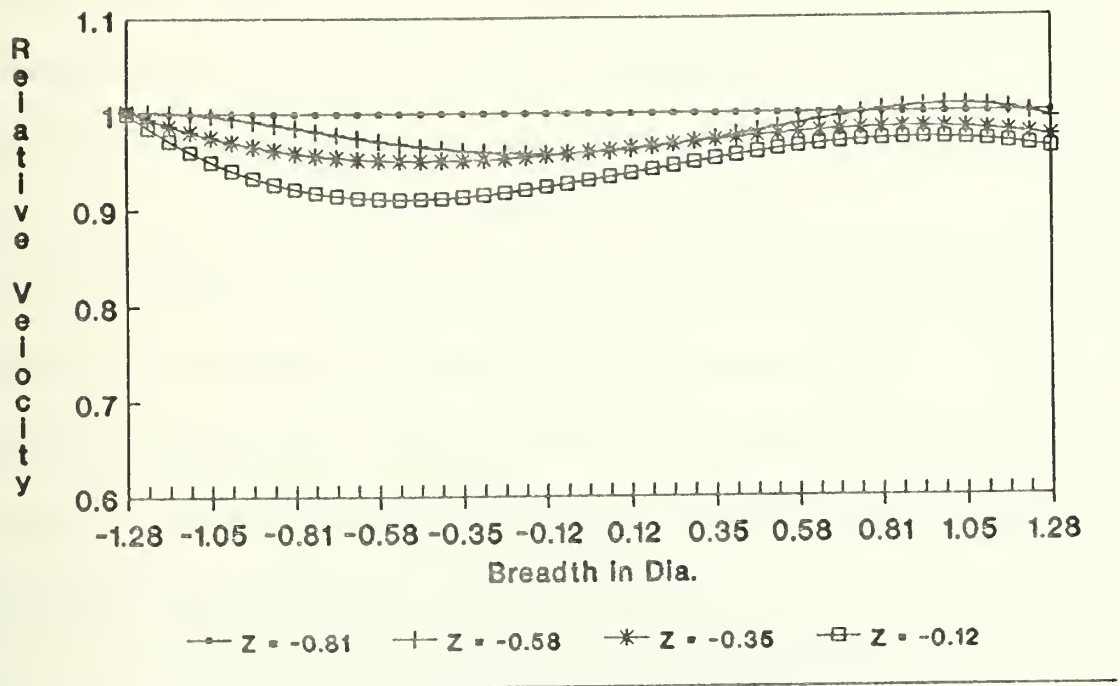

Figure 3.20 Selected profiles of wake five.

3.3 Discussion of Results

Wakes one, three, and four show good agreement on the general shape of the wake measured. Wake two does not show a symmetrical form nor does it fit the trend of wake development shown in wakes one and three. This data shows the effect of nonlinear drift that is not compensated for in the calibration procedure and is considered unreliable. Wake two is the average of two entirely separate wake measurements. The same measurements were repeated when preliminary results revealed the asymmetric pattern. This average did not improve the results and limits on tank availability prevented further measurements. Wake Five is the only wake measured on the surface and stands alone.

The common characteristics that are included in wakes one and three are a symmetry about the centerline of the sphere (breadth = 0), maximum wake deficits close to the free surface and velocities returning to the free stream below the sphere and away from the centerline. The effect of increasing X can be seen by comparing wakes one and three. The maximum wake deficit is almost the same for both wakes (0.84) suggesting that the maximum deficit is a weak function of X as is expected from the observation of wakes far behind ships in the open ocean. The breadth of the velocity deficit expands near the free surface as X increases and a smoother transition to the free stream is shown. Figure 3.21 compares the centerline profiles (Y = 0) of wakes one, three and four. This figure shows the wake deficit increasing at the free surface as X increases. This is interesting since it shows that the presence

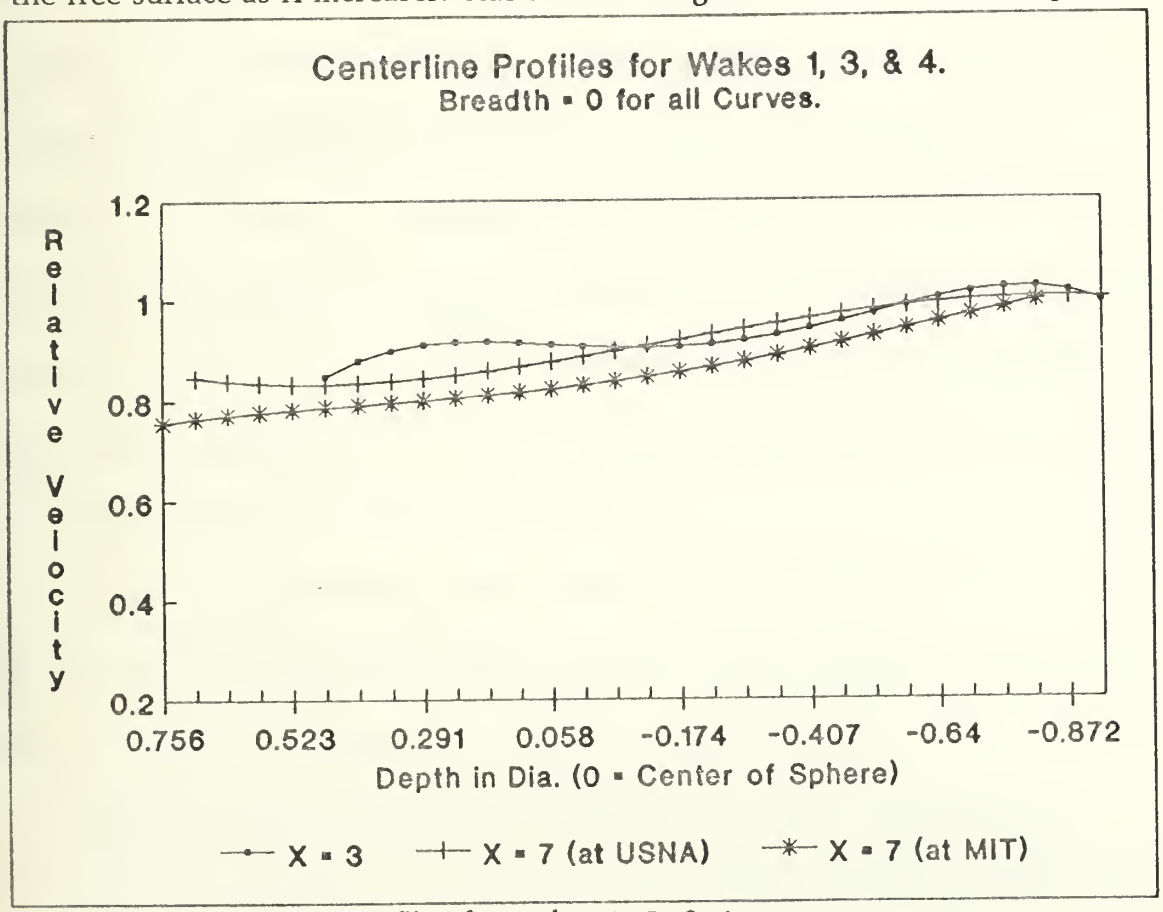

Figure 3.21 Centerline profiles for wakes 1, 3, & 4.

of the free surface drastically reduces the transfer of momentum in the vertical direction. As a result the turbulent wake close to the free surface spreads almost like a two-dimensional wake, one without vertical motion.

Wake four was assumed to have symmetric distribution around the centerline and only half of the wake profile is shown. This wake can be compared to wake three. The only difference in experimental procedure was that wake four was at a slightly higher absolute speed (0.930 vs 0.927 fps) than wake three due to limitations in speed control of the carriage. The more detailed measurements made for wake four show the maximum wake deficit to extend for a greater breadth and tapering off more quickly to the free stream velocity. The total breadth of the wake is the same in both wakes. The most interesting difference is the higher maximum wake deficit. The maximum wake deficit on the centerline is 0.78 vs 0.84 a 7% decrease which is reasonably close. Wake four had a little dip away from the centerline at Y = 0.45 with the maximum deficit of the entire wake measuring 0.70 vs 0.86 at the same point in wake three. This dip was the result of the more detailed measurements taken at MIT. This difference can be attributed in part to the higher speed at MIT, suggesting that the wake deficit is a very strong function of speed, but the nonlinear drift error could also be a factor.

This point illustrates the need for reducing the drift error in these experiments. Is this dip and the higher wake deficits really wake characteristics or error in the data? At this point, there is not enough information to say for sure.

Wake five shows much smaller overall dimensions when compared to the other wakes measured. This is expected with less of the sphere in the water. The

symmetry is skewed a little to the side though not as bad as shown in wake two. The same measurements were made in breadth for wakes four and five, but due to the lack of convincing symmetry the entire wake was plotted and not just half as in wake four. Additionally, the surface wake appears less smooth than the submerged wake, suggesting that the free surface contributes significantly to the dynamics within the wake.

Chapter 4: CONCLUSIONS AND RECOMMENDATIONS FOR FUTURE STUDY

The data presented in this thesis supports the feasibility of using hot film probes for measuring far field wake velocity profiles in a towing tank. The main conclusion that can be drawn from the measurements reported here is that the vicinity of the free surface drastically alters the form of a viscous wake. This is due to the fact that vertical momentum transfer is suppressed by the free surface, and the wake is diffused horizontally. As a result, visible horizontal velocity shear exists close to the free surface which is not present in the unbounded, three dimensional domains where momentum transfer is equal in all radial directions.

The data presented here can be used as inputs to instability computations and compared with numerical simulations. This data can also serve as a starting point for study of surface ships or submarines wakes using actual ship models.

In order to extend the range of X over which measurements are taken it is necessary to further reduce experimental errors. The use of temperature compensated hot film probes[14], though more expensive, would reduce the error imposed by temperature variations in the tank. The drift error is a more difficult problem to attack. Two factors should be considered; one is treating the water to eliminate or reduce the amount of drift, and the other is to reduce the time required to take the wake measurements.

Treatment of the tank water (chemical, thermal, or something else) was not tried, but is suggested as the most probable area for successful improvements based

---

[14]Lomas, p. 73-77.

on the idea that an insulating film is building up on the probes when in the water. An automated depth adjustment system and improved data collection capability would enable multiple depth measurements to be made on a single carriage run thereby reducing the total number of runs and the time spent waiting for the tank to return to equilibrium. Such a system could easily reduce the wake measurement time by 1/2 to 2/3.

An accurate flow meter could be used for calibration of the probes, thus eliminating the time needed to wait between calibration runs. The meter would have to be used with the probes installed on the carriage to eliminate errors caused by variations in probe alignment. To actually be faster than the carriage when using 7 or 8 probes the flow meter would have to be a multichannel device or be capable of quick easy measurements.

Two or three dimensional velocity components can be measured with hot film probes, using two component "X" probes or three component probes.[15] These probes require more elaborate electronic control packages than single wire probes and also need integrated data collection, calibration, and analysis systems.

---

[15] Hot Wire/Hot Film Anemometry Probes & Accessories, TSI Incorporated, (1983) pp. 21-25.

List of References

Bearman, P. W. "Corrections for the Effect of Ambient Temperature Drift on Hot Wire Measurements in Incompressible Flow." DISA Info., 1971.

Elachi, Charles. "Radar Images of the Earth from Space." Scientific American, December 1982.

Fry, D. J., and Y. H. Kim. "Bow Flow Fields of Surface Ships." Proc. 15th Symposium on Naval Hydrodynamics, 1985.

King, L. V. "On the Convection of Heat from Small Cylinders in a Stream of Fluid: Determination of the Convection Constants of Small Platinum Wires with Applications to Hot-Wire Anemometry." Phil. Trans. Roy. Soc., 1914.

Lomas, Charles G. Fundamentals of Hot Wire Anemometry. New York: Cambridge University Press, 1986.

Schlichting, Hermann. Boundary-Layer Theory. 7th ed. New York: McGraw-Hill Book Co., 1979.

Stefanick, Tom. "The Nonacoustic Detection of Submarines." Scientific American, March 1988, pp. 41-47.

Triantafyllou, George S. "Three Dimensional Instability Modes of the Wake Far Behind a Ship." Proc. 18th ONR Symposium on Naval Hydrodynamics. Ann Arbor, MI, (to appear), 1990.

TSI Incorporated. Hot Wire/Hot Film Anemometer Systems & Accessories. St. Paul, MN 1985.

TSI Incorporated. Hot Wire/Hot Film Anemometry Probes & Accessories. St. Paul, MN 1983.

Appendix A: Summary of Calibration Regression Results

The following pages contain the slope, y intercept, standard errors, and average drift correction for the King's Law linear regression as described in chapter 2. Each calibration graph is not shown as there are over 40 curve fits and this many graphs would not present a useful summary of results. The value of "R Squared" is a common indice used for linear regression; the better the fit is to the data the closer it is to one. Most all the curves had a R Squared value very close to one. Values less than 0.6 usually indicate little correlation between the independent and dependent variables.

Some of the curves have different values for the No. of Observations. This is because some of the slow velocity runs were below the maximum wake deficit and were eliminated from the regression analysis. This reduced the range of the linear curve fit and increased the accuracy of the fit over the region of wake measurements. This selective elimination of calibration points increased the R Squared values.

Wake two is the average of two separate profiles and the calibration data shown is that used for the first profile measurement. The second measurement was made just after wake one and the regression data in table A.1 was used.

Wakes four and five were both measured in two separate runs with different breadth values and two sets of calibration data for each wake. The corresponding breadth values are listed in the appropriate table.

The average drift values were more consistent for the data taken at USNA (wakes one to three) than at MIT. This is due to the much longer time that the

probes were left in the water to reduce the effect of drift. It should be noted that the slope of the calibration curves from USNA were much less than at MIT. This is also the result of leaving the probes in the water for a long time. The two results counter act one another. The more consistent the drift the less the experimental error and the lower the slope the greater velocity error caused by a variation in the voltage readings.

Table A.1 Summary of Calibration Regression Results for Wake One.

Regression Output:	PROBE 1	PROBE 2	PROBE 3	PROBE 4	PROBE 5
Y Intercept in $Volts^2$.	8.684	8.900	7.064	9.295	8.0428
Std Err of Y Est	0.0345	0.0443	0.0378	0.0358	0.0379
R Squared	0.9992	0.9990	0.9996	0.9991	0.9989
No. of Observations	8	8	8	8	8
Degrees of Freedom	6	6	6	6	6
Slope in $\frac{volts^2}{\sqrt{fps}}$.	7.949	8.728	12.860	7.938	7.200
Std Err of Slope	0.0901	0.1155	0.0988	0.0936	0.0989
Average drift correction in $\frac{Volts}{Min}$.	$3.79e^{-4}$	$4.34e^{-4}$	$1.167e^{-3}$	$3.42e^{-4}$	$3.41e^{-4}$

Table A.2 Summary of Calibration Regression Results for Wake Two. (First of two measurements, second used same calibration data as wake one.)					
Regression Output:	PROBE 1	PROBE 2	PROBE 3	PROBE 4	PROBE 5
Y Intercept in $Volts^2$.	9.3862	9.5948	8.0314	9.8261	8.7314
Std Err of Y Est	0.0211	0.0313	0.0662	0.0424	0.0239
R Squared	0.9998	0.9995	0.9991	0.9990	0.9996
No. of Observations	8	8	8	8	8
Degrees of Freedom	6	6	6	6	6
Slope in $\frac{Volts^2}{\sqrt{fps}}$.	8.7362	9.5258	14.4991	8.5216	7.5686
Std Err of Slope.	0.0559	0.0829	0.1753	0.1123	0.0634
Average drift correction in $\frac{Volts}{Min}$.	$5.67e^{-4}$	$5.46e^{-4}$	$7.55e^{-4}$	$4.39e^{-4}$	$4.26e^{-4}$

Table A.3 Summary of Calibration Regression Results for Wake Three.					
Regression Output:	PROBE 1	PROBE 2	PROBE 3	PROBE 4	PROBE 5
Y intercept in $Volts^2$.	9.0019	9.2661	7.8970	9.5716	8.3882
Std Err of Y Est	0.0341	0.0568	0.0550	0.0532	0.0362
R Squared	0.9993	0.9983	0.9993	0.9982	0.9990
No. of Observations	8	8	8	8	8
Degrees of Freedom	6	6	6	6	6
Slope in $\frac{Volts^2}{\sqrt{fps}}$.	8.1559	8.8968	13.2217	8.0196	7.2423
Std Err of slope.	0.0895	0.1491	0.1443	0.1395	0.0951
Average drift correction in $\frac{Volts}{Min}$.	$2.51e^{-4}$	$2.57e^{-4}$	$5.68e^{-4}$	$1.81e^{-4}$	$2.08e^{-4}$

Table A.4 Summary of Calibration Regression Data for Wake Four.
(Breadth = ±1.28, ±0.81, ±0.35, and 0 dia.)

Reg. Output	PROBE 1	PROBE 2	PROBE 3	PROBE 4	PROBE 5	PROBE 6	PROBE 7
Y inter in $Volts^2$.	8.9606	9.3099	8.9727	8.9573	13.406	7.3778	3.0794
Std Err of Y Est	0.0707	0.0737	0.0442	0.0657	0.0578	0.0388	0.0239
R^2	0.9931	0.9971	0.9970	0.9981	0.9972	0.9990	0.9944
No. of Obser.	6	7	4	7	6	7	5
Deg. of Freed.	4	5	2	5	4	5	3
Slope in $\frac{Volts^2}{\sqrt{fps}}$	9.5001	13.696	13.163	15.045	12.207	12.702	3.9189
Std Err of Slope.	0.3947	0.3330	0.5098	0.2967	0.3227	0.1754	0.1698
Ave. drift correction in $\frac{Volts}{Min}$.	$1.28e^{-3}$	$1.72e^{-3}$	$1.71e^{-3}$	$-0.05e^{-3}$	$-0.27e^{-3}$	$1.33e^{-3}$	$-0.03e^{-3}$

Table A.5 Summary of Calibration Regression Results for Wake Four. (Breadth = -0.23, 0, 0.23, 0.58, 0.93, 1.28 dia.)						
Regression Output:	PROBE 1	PROBE 2	PROBE 3	PROBE 4	PROBE 5	PROBE 6
Y intercept in $Volts^2$	11.550	7.7370	9.4305	13.178	7.9561	2.7245
Std Err of Y Est	0.0425	0.0396	0.0832	0.0741	0.1082	0.0234
R Squared	0.9982	0.9992	0.9974	0.9978	0.9946	0.9976
No. of Observations	6	7	7	7	7	7
Degrees of Freedom	4	5	5	5	5	5
Slope in $\frac{volts^2}{\sqrt{fps}}$	11.124	14.422	16.496	15.892	14.820	4.8140
Std Err of Slope	0.2369	0.1790	0.3756	0.3347	0.4886	0.1058
Average drift correction in $\frac{Volts}{\text{min}}$.	$1.77e^{-3}$	$1.73e^{-3}$	$1.83e^{-3}$	$2.69e^{-3}$	$1.00e^{-3}$	$0.17e^{-3}$

Table A.6 Summary of Calibration Regression Data for Wake Five. (Breadth = ±1.28, ±0.81, ±0.35, and 0 dia.)							
Regression Output:	PROBE 1	PROBE 2	PROBE 3	PROBE 4	PROBE 5	PROBE 6	PROBE 7
Y inter. in $Volts^2$.	9.2062	8.3205	6.3053	9.0437	11.625	6.8840	3.4619
Std Err of Y Est	0.0426	0.0751	0.0384	0.0642	0.0691	0.0764	0.0136
R Squared	0.9990	0.9977	0.9971	0.9978	0.9983	0.9979	0.9993
No. of Observa-tions	6	6	7	6	6	7	7
Degrees of Free.	4	4	5	4	4	5	5
Slope in $\frac{volts^2}{\sqrt{fps}}$	15.000	17.593	7.1355	15.200	18.784	16.664	5.2302
Std Err of Slope.	0.2376	0.4187	0.1734	0.3580	0.3852	0.3449	0.0613
Average drift correc-tion in $\frac{Volts}{Min}$	$2.88e^{-3}$	$1.67e^{-3}$	$1.89e^{-4}$	$2.68e^{-3}$	$4.16e^{-3}$	$1.15e^{-3}$	$1.97e^{-4}$

Table A.7 Summary of Calibration Regression Results for Wake Five. (Breadth = -0.23, 0, 0.23, 0.58, 0.93, 1.28 dia.)						
Regression Output:	PROBE 1	PROBE 2	PROBE 3	PROBE 4	PROBE 5	PROBE 6
Y intercept in $Volts^2$.	10.3341	6.2610	9.5331	11.771	6.6857	3.1007
Std Err of Y Est	0.0537	0.0512	0.0403	0.0992	0.0202	0.0238
R Squared	0.9981	0.9990	0.9992	0.9961	0.9998	0.9979
No. of Observations	6	6	6	6	5	7
Degrees of Freedom	4	4	4	4	3	5
Slope in $\frac{volts^2}{\sqrt{fps}}$	13.555	18.009	15.643	17.629	16.729	5.2592
Std Err of Slope.	0.2994	0.2854	0.2251	0.5535	0.1440	0.1073
Average drift correction in $\frac{Volts}{Min}$.	2.45^{-3}	$2.25e^{-3}$	$2.81e^{-3}$	$3.55e^{-3}$	$1.43e^{-3}$	$1.40e^{-4}$

Appendix B: Summary of Velocity Measurements

This appendix contains tables summarizing the actual velocity measurements used to develop the graphs presented in chapter 3. The names of wake one, wake two, etc. correspond to the names in chapter 3. The breadth (Y) and depth (Z) positions are in diameters of the sphere. The velocity values have been normalized by the free stream velocity as noted on the tables. Thus, the wakes can be thought of as a velocity deficit behind the sphere.

In tables B.1 through B.3, the probe numbers correspond to the numbers listed in Appendix A. Tables B.3 and B.4 do not have probe numbers listed as they are the combination of two separate wake measurements and the continuity of the numbering system was lost when these measurements were combined.

The velocity values of 1.000 for the deepest measurements (most negative Z) in all tables are a result of the assumption that these measurements were in the free stream. These points were used as a reference to refine the drift correction as described in chapter 3. Thus, they do not represent a true measurement of wake velocity.

Table B.1 Summary of Velocity Measurements for Wake One. (Velocity normalized by free stream = 0.926 fps)					
Depth (Z) in Dia.	PROBE 1	PROBE 2	PROBE 3	PROBE 4	PROBE 5
	Y = -0.81	Y = -0.35	Y = 0	Y = 0.35	Y = 0.81
-0.93	1.000	1.000	1.000	1.000	1.000
-0.70	0.991	1.000	0.994	0.999	0.994
-0.47	0.986	0.994	0.981	1.000	0.996
-0.23	0.972	0.986	0.913	0.987	0.993
0	0.968	0.988	0.880	0.985	0.991
0.23	0.960	0.878	0.938	0.945	0.991
0.47	1.001	0.828	0.843	0.950	0.993

Table B.2 Summary of Velocity Measurements for Wake Two. (Velocity normalized by free stream = 0.926 fps)					
Depth (Z) in dia.	PROBE 1	PROBE 2	PROBE 3	PROBE 4	PROBE 5
	Y = -0.81	Y = -0.35	Y = 0	Y = 0.35	Y = 0.81
-0.93	1.000	1.000	1.000	1.000	1.000
-0.70	0.999	1.000	0.999	0.998	0.999
-0.47	0.981	0.992	0.996	0.995	1.000
-0.23	0.961	0.967	0.967	0.991	0.998
0.00	0.918	0.916	0.931	0.975	0.988
0.23	0.920	0.920	0.922	0.959	0.984
0.47	0.910	0.881	0.904	0.942	0.983

Table B.3 Summary of Velocity Measurements for Wake Three.
(Velocity normalized by free stream = 0.926 fps.)

Depth (Z) in dia.	PROBE 1	PROBE 2	PROBE 3	PROBE 4	PROBE 5
	Y = -0.81	Y = -0.35	Y = 0	Y = 0.35	Y = 0.81
-0.93	1.000	1.000	1.000	1.000	1.000
-0.70	0.993	0.996	0.999	0.999	0.999
-0.47	0.989	0.984	0.969	0.993	0.994
-0.23	1.001	1.001	0.935	1.001	0.973
0.00	0.975	0.967	0.876	0.989	0.948
0.23	0.971	0.949	0.867	0.975	0.940
0.47	0.920	0.890	0.824	0.964	0.905
0.70	0.849	0.837	0.759	0.923	0.857

Table B.4 Summary of Velocity Measurements for Wake Four.
(Velocities normalized by free stream = 0.930 fps)[16]

Depth (Z) in dia.	Y = 0	Y = 0.23	Y = 0.35	Y = 0.58	Y = 0.81	Y = 0.93	Y = 1.28
-0.81	1.000	1.000	Del.	1.000	1.000	1.000	1.000
-0.58	0.927	0.998	1.000	0.998	0.997	0.998	0.989
-0.35	0.899	0.939	Del.	0.962	0.994	0.996	0.985
-0.12	0.871	0.893	0.987	Del.	Del.	0.994	0.982
0.00	0.822	0.774	0.919	Del.	1.021	0.959	0.974
0.12	0.804	0.807	Del.	0.808	0.731	0.963	0.876
0.35	0.805	0.776	Del.	0.732	0.997	0.921	0.971
0.58	0.779	0.701	Del.	0.679	0.994	0.894	0.961
0.81	0.747	0.703	Del.	0.658	1.002	0.918	0.963

[16]Entries marked "Del." were deleted as unreasonable in relation to the other values measured around them. Probe 3 appears to be faulty.

Table B.5 Summary of Velocity Measurements for Wake Five. (Velocity normalized by free stream = 0.930 fps.)				
Breadth (Y)in dia.	Z = -0.81	Z = -0.58	Z = -0.35	Z = -0.12
-1.28	1.000	1.000	0.999	0.998
-0.81	1.000	0.993	0.974	0.932
-0.35	1.000	0.977	0.955	0.912
-0.23	1.000	0.918	0.911	0.889
0.00	1.000	0.972	0.978	0.955
0.23	1.000	0.971	0.963	0.930
0.35	1.000	0.978	1.000	0.966
0.58	1.000	1.000	0.978	0.982
0.81	1.000	0.993	0.975	0.944
0.93	1.000	1.000	0.978	0.982
1.28	1.000	0.998	0.979	0.965

Appendix C: Examples of Data Processing Calculations.

The following two pages contain examples of calibration curve fit and wake measurement calculations. The data shown is for a single probe that was used in measuring wake three. Explanatory notes are included with the listed calculations. A complete list of all calculations would be redundant and excessive. The results are summarized in Appendices A and B.

PROBE1 CALIBRATION FOR WAKE THREE

Second Calibration Run

Kings Law Exponent n = 0.5

1	2	3	4	5	6	7	8	9	10	11
Avg volts	Water temp	Volts cor	Drift fac	Time dif	Drift cor	Avg col 6 & 6a	Col 7 Sqrd	Col 6 Sqrd	Carriage speed^n	Regres pts
3.782	20.78	3.785	2.384E-04	0	3.785	3.787	14.338	14.330	0.654	14.332
3.856	20.78	3.860	2.448E-04	6	3.861	3.861	14.910	14.909	0.722	14.890
3.923	20.78	3.927	2.428E-04	12	3.930	3.930	15.445	15.441	0.796	15.498
3.986	20.78	3.990	2.412E-04	19	3.994	3.995	15.956	15.955	0.852	15.950
4.047	20.77	4.050	2.463E-04	24	4.056	4.056	16.449	16.450	0.908	16.408
4.095	20.77	4.098	2.618E-04	30	4.105	4.103	16.836	16.852	0.965	16.869
4.154	20.77	4.157	2.653E-04	36	4.166	4.163	17.333	17.355	1.018	17.307
4.195	20.77	4.198	2.721E-04	42	4.209	4.205	17.683	17.713	1.066	17.695
	Average drift =		2.516E-04							

Third Calibration Run

1a	2a	3a	5a	6a	9a
ave volts	Water temp	Volts cor	Time dif	Drift cor	Col 6a Sqrd
3.722	20.74	3.724	254	3.788	14.345
3.795	20.74	3.796	260	3.862	14.912
3.862	20.74	3.863	266	3.930	15.448
3.925	20.73	3.926	271	3.995	15.957
3.985	20.73	3.986	277	4.056	16.448
4.028	20.74	4.030	282	4.101	16.819
4.087	20.74	4.088	287	4.161	17.311
4.126	20.74	4.128	292	4.201	17.652

Regression Output:

Y intercept	9.0019
Std Err of Y Est	0.0341
R Squared	0.9993
No. of Observations	8.0000
Degrees of Freedom	6.0000
Slope	8.1559
Std Err of Slope.	0.0895

NOTES:

1. Columns 1, 1a, 2, 2a, 5, & 5a are all inputs.
2. Columns 3 & 3a correct ave volts to reference temp of 20.7 degrees C.
3. Column 4 subtracts col 1a from col 1 and divides by the time between calibration runs (252.5 min).
4. Columns 6 & 6a are corrected voltages for drift.
   Average drift is multiplied by col 5 & 5a and added to col 3 & 3a respectively.
5. Regression analysis used col 8 as the dependent variable and col 10 as independent variable.
6. Column 11 lists the voltage squared values predicted by the regression curve fit.
7. Columns 8, 9, 9a, & 11 can all be compared to assess the curve fit.

MEASUREMENTS FOR WAKE THREEE (at X = 7 Dia. and sphere submerged 1 Dia.)

PROBE 1 (Y = -0.81 dia.) Speed = 0.9266 FPS

1	2	3	4	5	6	7	8	9	10
Avg volts	Water temp	Volts cor	Time dif	Drift cor	col 5 Sqrd	Depth (Z) in dia.	Wake vel	Rel Vel	Adj Vel
4.092	20.76	4.094	81	4.107	16.870	-0.93	0.931	1.004	1.000
4.086	20.75	4.089	94	4.104	16.840	-0.70	0.924	0.997	0.993
4.082	20.75	4.084	110	4.102	16.826	-0.47	0.920	0.993	0.989
4.077	20.74	4.079	178	4.108	16.872	-0.23	0.931	1.005	1.001
4.067	20.74	4.068	190	4.099	16.802	0.00	0.915	0.979	0.975
4.054	20.73	4.055	226	4.092	16.741	0.00	0.900	0.975	0.971
4.059	20.74	4.061	202	4.093	16.755	0.23	0.904	0.924	0.920
4.032	20.73	4.034	214	4.068	16.549	0.47	0.856	0.853	0.849
3.992	20.73	3.993	238	4.031	16.253	0.70	0.790		

Regression Output:

Y intercept	9.0019	Average Drift = 2.516E-04
Std Err of Y Est	0.0341	
R Squared	0.9993	
No. of Observations	8.0000	
Degrees of Freedom	6.0000	
Slope	8.1559	
Std Err of Slop	0.0895	

NOTES:

1. Columns 1, 2, 4, & 7 are all input.
2. Column 3 correct avg volts to reference temp of 20.7 degrees C.
3. Column 5 corrects col 3 for drift using the average drift and velocity adjustment in col 10.
   First the avg drift is multiplied by col 4 and added to col 3.
   Then the avg drift is reduced (9E-5 in this case) to lower any values above 1.0 in col 9 to 1.0.
   This is an iterative process. Col 10 is first calculated using the avg drift then the reduction is determined.
4. Column 8 uses the regression output to convert col 6 from a voltage to a velocity.
5. Column 9 averages any repeat measurements and divides by the free stream velocity.
6. Column 10 subtracts a constant value from col 9 to force the deepest measurement to equal the free stream.

Appendix D: Listing of Surface Fit Program

The following program was written by LCDR Frank Camelio as part of his research using hot wire X probes in the MIT acoustic and vibration laboratory. The program fits a polynomial surface using 25 coefficients through data consisting of two independent variables and one dependent variable. The program also calculates a summary of errors to assess the quality of the curve fit and generates an output file to use in the plotting the surface.

```
c*****************************************************************
c     This program reads velocity-angle-voltage data or stream
c     and vertical velocity data and fits separately a double
c     polynomial surface, one in velocity and one in angle OR
c     one in u-velocity and one in v-velocity, to voltage data
c     on both channels of an X-probe.  The data is obtained from
c     a calibration which pivots the probe at different positive
c     and negative angles with respect to the free stream.
c     Polynomial order is either 3, giving 16 coefficients, or
c     4, giving 25 coefficients.
c     The 2-d polynomial format is:
c                N   N
c     f(e1,e2)=SUM SUM a(i,j)*e1**(j-1)*e2**(i-1)  [N=4 or 5]
c              i=1 j=1
c
c     where e1,e2 are channel voltages and a(i,j) are the fitted
c     coefficients.  For simplicity in analysis coefficients are
c     transferred to vector format vice an array.
c*****************************************************************

      program xcoeff

      implicit real*8 (a-h,o-z)
      real*8 qu(200,1),av(200,1)
      real*8 quest(200),qudel(200),avest(200),avdel(200)
      real*8 etqu(25,1),etav(25,1),qufest(200),avfest(200)
      real*8 ee(200,25),eet(25,200),ete(25,25)
      real*8 qumaxerr,quaverr,qusumerr,quvarsum,quvar
      real*8 avmaxerr,avaverr,avsumerr,avvarsum,avvar
      real*8 qurel(200),avrel(200)

      character*15 name,fileout1,fileout2

      common /arry/ xx(25,27),ix(25)
      common /xco/ e1(200),e2(200)
      common /funcalc/ ao(25),bo(25)
      real qu16,av16,qu25,av25
      external qu16,av16,qu25,av25

50    write(6,*) 'Enter name of calibration data file.'
      read(5,*) name
      write(6,*)

c*****************************************************************
c     READ VALUES FROM Q-A OR U-V CALIBRATION .DAT FILE
c*****************************************************************

      open(51,file=name,status='old')
      m=1
100     read(51,*,end=150) e1(m),e2(m),qu(m,1)
      m=m+1
      goto 100
150   close(51)
      m=m-1

      write(6,*) 'Enter 1 if data is q-a, 2 if u-v.'
      read(5,*) num2
      write(6,*)
200   write(6,*) 'Enter # of coefficients to fit (INTEGER).'
      read(5,*) num1
      write(6,*)

      if (num1.eq.16.and.num2.eq.1) then
        fileout1='x16coqa.dat'
        fileout2='x16coqa.fmt'
      endif
```

```
      if (num1.eq.16.and.num2.eq.2) then
        fileout1='randy16.dat'
        fileout2='randy16.fmt'
      endif

      if (num1.eq.25.and.num2.eq.1) then
        fileout1='x25coqa.dat'
        fileout2='x25coqa.fmt'
      endif

      if (num1.eq.25.and.num2.eq.2) then
        fileout1='randy25.dat'
        fileout2='randy25.fmt'
      endif

      open(7,file=fileout1,status='fresh')
      open(8,file=fileout2,status='fresh')

      if(num2.eq.1) write(8,*) '    q coeff','        a coeff'
      if(num2.eq.2) write(8,*) '    u coeff','        v coeff'

300   if (num1.eq.16) call coeff16(m,ee)
      if (num1.eq.25) call coeff25(m,ee)

      do 400 i=1,m
        do 400 j=1,num1
400   eet(j,i)=ee(i,j)

      call matmlt(eet,ee,ete,num1,m,num1)
      call matmlt(eet,qu,etqu,num1,m,1)

      do 500 i=1,num1
        do 500 j=1,num1
500   xx(i,j)=ete(i,j)

      do 600 i=1,num1
600     xx(i,num1+1)=etqu(i,1)

      call algr(num1,1,1,e)

      do 700 i=1,num1
        ao(i)=xx(i,num1+1)
        write(6,*) ao(i)
        write(7,*) ao(i)
700     write(8,*) ao(i)
      write(8,*)
      write(8,*)
      close(7)

c*************************************************************
c     ERROR ANALYSIS
c*************************************************************

      write(8,*)
      if(num2.eq.1) then
      write(8,*) '  q-act  ','  q-fit  ','q-funct '
     &,' delta-q',' q rel err'
      endif
      if(num2.eq.2) then
      write(8,*) '  u-act  ','  u-fit  ','u-funct '
     &,' delta-u',' u rel err'
      endif

      do 800 i=1,m
        if(num1.eq.16) qufest(i)=qu16(e1(i),e2(i))
```

```
            if(num1.eq.25) qufest(i)=qu25(el(i),e2(i))
            quest(i)=0
            do 750 j=1,num1
  750         quest(i)=quest(i)+ao(j)*ee(i,j)
            qudel(i)=qu(i,1)-quest(i)
            if(qu(i,1).eq.0.) then
               qurel(i)=0.
            else
               qurel(i)=100*qudel(i)/qu(i,1)
            endif
            if(qurel(i).eq.0.) then
             write(8,760) qu(i,1),quest(i),qufest(i),qudel(i)
  760         format(4f9.5,3x)
            else
             write(8,770) qu(i,1),quest(i),qufest(i),qudel(i),qurel(i)
  770         format(5f9.5,3x)
            endif
            if(i.eq.1) qumaxerr=abs(qudel(i))
            qumaxerr=max(abs(qudel(i)),qumaxerr)
  800     continue
          write(8,*)

          qusumerr=0
          do 900 i=1,m
  900       qusumerr=qusumerr+abs(qudel(i))
          quaverr=qusumerr/dble(m)
          quvarsum=0
          do 1000 i=1,m
  1000      quvarsum=quvarsum+(abs(qudel(i))-quaverr)**2
          quvar=quvarsum/dble(m)

          write(8,*)
          if(num2.eq.1) then
           write(8,*) 'Max q vel error magnitude (m/sec) = ',qumaxerr
           write(8,*) 'Avg q vel error magnitude (m/sec) = ',quaverr
           write(8,*) 'Var q vel error magnitude (m/sec) = ',quvar
          endif
          if(num2.eq.2) then
           write(8,*) 'Max u vel error magnitude (m/sec) = ',qumaxerr
           write(8,*) 'Avg u vel error magnitude (m/sec) = ',quaverr
           write(8,*) 'Var u vel error magnitude (m/sec) = ',quvar
          endif

          write(6,*) 'Enter 3 to change # coefficients.'
          write(6,*) 'Enter 4 to change q-a to u-v or vice-versa.'
          write(6,*) 'Else enter any other integer.'
          read(5,*) num3
          write(6,*)
          if(num3.eq.3) goto 200
          if(num3.eq.4) goto 50

          close(8)

          stop
          end

c*****************************************************************
c     SUBROUTINES - PRODUCTS OF VOLTAGES (16 AND 25 COEFF's)
c*****************************************************************

          subroutine coeff16(m,ee)

          implicit real*8 (a-h,o-z)
          dimension ee(200,25)
          common /xco/ el(200),e2(200)
```

```
      do 10 i=1,m
        ee(i,1)=1
        ee(i,2)=e1(i)
        ee(i,3)=e1(i)*e1(i)
        ee(i,4)=e1(i)*ee(i,3)
        ee(i,5)=e2(i)
        ee(i,6)=e2(i)*e1(i)
        ee(i,7)=e2(i)*ee(i,3)
        ee(i,8)=e2(i)*ee(i,4)
        ee(i,9)=e2(i)*e2(i)
        ee(i,10)=e2(i)*ee(i,6)
        ee(i,11)=e2(i)*ee(i,7)
        ee(i,12)=e2(i)*ee(i,8)
        ee(i,13)=e2(i)*ee(i,9)
        ee(i,14)=e2(i)*ee(i,10)
        ee(i,15)=e2(i)*ee(i,11)
        ee(i,16)=e2(i)*ee(i,12)
10    continue

      return
      end

c*********************************************************************

      subroutine coeff25(m,ee)

      implicit real*8 (a-h,o-z)
      dimension ee(200,25)
      common /xco/ e1(200),e2(200)

      do 10 i=1,m
        ee(i,1)=1
        ee(i,2)=e1(i)
        ee(i,3)=e1(i)*e1(i)
        ee(i,4)=e1(i)*ee(i,3)
        ee(i,5)=e1(i)*ee(i,4)
        ee(i,6)=e2(i)
        ee(i,7)=e2(i)*e1(i)
        ee(i,8)=e2(i)*ee(i,3)
        ee(i,9)=e2(i)*ee(i,4)
        ee(i,10)=e2(i)*ee(i,5)
        ee(i,11)=e2(i)*ee(i,6)
        ee(i,12)=e2(i)*ee(i,7)
        ee(i,13)=e2(i)*ee(i,8)
        ee(i,14)=e2(i)*ee(i,9)
        ee(i,15)=e2(i)*ee(i,10)
        ee(i,16)=e2(i)*ee(i,11)
        ee(i,17)=e2(i)*ee(i,12)
        ee(i,18)=e2(i)*ee(i,13)
        ee(i,19)=e2(i)*ee(i,14)
        ee(i,20)=e2(i)*ee(i,15)
        ee(i,21)=e2(i)*ee(i,16)
        ee(i,22)=e2(i)*ee(i,17)
        ee(i,23)=e2(i)*ee(i,18)
        ee(i,24)=e2(i)*ee(i,19)
        ee(i,25)=e2(i)*ee(i,20)
10    continue

      return
      end

c*********************************************************************
c     SUBROUTINES - MATRIX MULTIPLICATION, SIMUL EQN SOLUTION
c*********************************************************************

      subroutine matmlt(aa,u,t,mm,nn,pp)
```

```
      real*8 aa(25,200),u(200,25),t(25,25)
      integer pp

      do  1 i=1,mm
        do 1 j=1,pp
1       t(i,j)=0

      do 2 i=1,mm
        do 2 j=1,pp
           do 2 k=1,nn
2          t(i,j)=aa(i,k)*u(k,j)+t(i,j)

      return
      end

c*********************************************************************
c
c algr solve a real algebraic system
c
c id=1: reduce, solve for nr right hand sides
c id=0, nr>0:   solve for nr right hand sides
c id=0, nr=0:   wielandt correction step
c id=-1: reduce, first wielandt step
c
c                   Kay Berbert 1987
c
c*********************************************************************

      subroutine algr(n,nr,id,e)
      implicit real*8 (a-h,o-z)
      common /arry/ a(25,27),ix(25)

      m=n+nr
      m1=n-1
      n1=n+1
      if (id.eq.0) go to 10
      do 1 k=1,m1
      xx=0.
      kx=k
      do 2 kk=k,n
      x=dabs(a(kk,k))
      if (x.le.xx) go to 2
      xx=x
      kx=kk
2     continue
      ix(k)=kx
      if (kx.eq.k) go to 3
      do 4 jj=k,m
      z=a(k,jj)
      a(k,jj)=a(kx,jj)
4     a(kx,jj)=z
3     continue
      k1=k+1
      do 1 kk=k1,n
      if (dabs(a(k,k)).le.0.) go to 1
      a(kk,k)=a(kk,k)/a(k,k)
      do 5 jj=k1,m
5     a(kk,jj)=a(kk,jj)-a(kk,k)*a(k,jj)
1     continue
      if (id.gt.0) go to 12

      a(n,n1)=1.
      do 6 kk=1,m1
      k=n-kk
      a(k,n1)=-a(k,n)
```

```
      if (k.eq.m1) go to 6
      k1=k+1
      do 7 l=k1,m1
7     a(k,n1)=a(k,n1)-a(k,l)*a(l,n1)
6     a(k,n1)=a(k,n1)/a(k,k)
      return

10    if (nr.le.0) m=n1
      do 11 l=n1,m
      do 11 k=1,m1
      kx=ix(k)
      z=a(k,l)
      a(k,l)=a(kx,l)
      a(kx,l)=z
      k1=k+1
      do 11 kk=k1,n
11    a(kk,l)=a(kk,l)-a(kk,k)*a(k,l)
      if (nr.gt.0) go to 12

      e=a(n,n)/a(n,m)
      do 13 k=1,n
13    a(k,m)=e*a(k,m)

12    if (m.le.n) return
      do 14 kk=1,n
      k=n1-kk
      if (k.eq.n) go to 15
      k1=k+1
      do 20 l=n1,m
      do 20 ll=k1,n
20    a(k,l)=a(k,l)-a(k,ll)*a(ll,l)
15    do 14 l=n1,m
14    a(k,l)=a(k,l)/a(k,k)
      return
      end

c**********************************************************************
ccc   FUNCTIONS TO CONVERT VOLTAGES TO VELOCITY AND ANGLE       ccc
**********************************************************************

      function qu16(v1,v2)

      implicit real*8 (e,f,v)
      common /funcalc/ e(25),f(25)

      qu16=e(1)+v1*(e(2)+v1*(e(3)+v1*e(4)))+
     &v2*(e(5)+v1*(e(6)+v1*(e(7)+v1*e(8)))+
     &v2*(e(9)+v1*(e(10)+v1*(e(11)+v1*e(12)))+
     &v2*(e(13)+v1*(e(14)+v1*(e(15)+v1*e(16))))))

      return
      end

c**********************************************************************

      function av16(v1,v2)

      implicit real*8 (e,f,v)
      common /funcalc/ e(25),f(25)

      av16=f(1)+v1*(f(2)+v1*(f(3)+v1*f(4)))+
     &v2*(f(5)+v1*(f(6)+v1*(f(7)+v1*f(8)))+
     &v2*(f(9)+v1*(f(10)+v1*(f(11)+v1*f(12)))+
     &v2*(f(13)+v1*(f(14)+v1*(f(15)+v1*f(16))))))

      return
```

```
      end
c*********************************************************************
      function qu25(v1,v2)

      implicit real*8 (g,h,v)
      common /funcalc/ g(25),h(25)

      qu25=g(1)+v1*(g(2)+v1*(g(3)+v1*(g(4)+v1*g(5))))+
     &v2*(g(6)+v1*(g(7)+v1*(g(8)+v1*(g(9)+v1*g(10))))+
     &v2*(g(11)+v1*(g(12)+v1*(g(13)+v1*(g(14)+v1*g(15))))+
     &v2*(g(16)+v1*(g(17)+v1*(g(18)+v1*(g(19)+v1*g(20))))+
     &v2*(g(21)+v1*(g(22)+v1*(g(23)+v1*(g(24)+v1*g(25)))))))

      return
      end
c*********************************************************************
      function av25(v1,v2)

      implicit real*8 (g,h,v)
      common /funcalc/ g(25),h(25)

      av25=h(1)+v1*(h(2)+v1*(h(3)+v1*(h(4)+v1*h(5))))+
     &v2*(h(6)+v1*(h(7)+v1*(h(8)+v1*(h(9)+v1*h(10))))+
     &v2*(h(11)+v1*(h(12)+v1*(h(13)+v1*(h(14)+v1*h(15))))+
     &v2*(h(16)+v1*(h(17)+v1*(h(18)+v1*(h(19)+v1*h(20))))+
     &v2*(h(21)+v1*(h(22)+v1*(h(23)+v1*(h(24)+v1*h(25)))))))

      return
      end
c*********************************************************************
```

```
c*************************************************************
c     PROGRAM USES CALIBRATION COEFFICIENTS AND PRODUCES
c     U(E1,E2) AND V(E1,E2) AT UNIFORM INTERVALS AND WRITES
c     DATA TO FILE FOR USE AS INPUT INTO SURFER (PC)
c     SOFTWARE.
c*************************************************************

      program uvmatrix

      character*15 fname

      common /ufunct25/ ai(25)
      common /vfunct25/ bi(25)
      external u25,v25

      write(6,*) 'Enter name of coefficients file.'
      read(5,*) fname
      open(51,file=fname,status='old')
      do 25 i=1,25
        read(51,*) ai(i)
25    continue
      close(51)

      write(6,*)
      write(6,*) 'Enter the starting value for E1 voltage.'
      read(5,*) vol1
      write(6,*)
      write(6,*) 'Enter the starting value for E2 voltage.'
      read(5,*) vol2
      write(6,*)
      write(6,*) 'Enter the maximum value for E1 voltage.'
      read(5,*) vol1max
      write(6,*)
      write(6,*) 'Enter the maximum value for E2 voltage.'
      read(5,*) vol2max
      write(6,*)
      write(6,*) 'Enter the INTEGER number of voltage intervals.'
      read(5,*) nint1
      write(6,*)
      write(6,*)
      step=(vol1max-vol1)/real(nint1)
      nint2=int(real(vol2max-vol2)/step)+1
      nint1=nint1+1

      open(7,file='rzmatrix.dat',status='fresh')

      do 100 j=1,nint2
        v2=vol2+real(j-1)*step
        do 50 i=1,nint1
           v1=vol1+real(i-1)*step
           u=u25(v1,v2)
           write(7,*) v1,v2,u
50    continue
100   continue

      close(7)
      stop
      end

*********************************************************************
ccc   FUNCTIONS TO CONVERT VOLTAGES TO VELOCITY AND ANGLE      ccc
*********************************************************************
      function u25(e1,e2)

      common /ufunct25/ a(25)
```

```
      u25=a(1)+e1*(a(2)+e1*(a(3)+e1*(a(4)+e1*a(5))))+
     &e2*(a(6)+e1*(a(7)+e1*(a(8)+e1*(a(9)+e1*a(10))))+
     &e2*(a(11)+e1*(a(12)+e1*(a(13)+e1*(a(14)+e1*a(15))))+
     &e2*(a(16)+e1*(a(17)+e1*(a(18)+e1*(a(19)+e1*a(20))))+
     &e2*(a(21)+e1*(a(22)+e1*(a(23)+e1*(a(24)+e1*a(25))))))))

      return
      end
c*****************************************************************
      function v25(e1,e2)

      common /vfunct25/ b(25)

      v25=b(1)+e1*(b(2)+e1*(b(3)+e1*(b(4)+e1*b(5))))+
     &e2*(b(6)+e1*(b(7)+e1*(b(8)+e1*(b(9)+e1*b(10))))+
     &e2*(b(11)+e1*(b(12)+e1*(b(13)+e1*(b(14)+e1*b(15))))+
     &e2*(b(16)+e1*(b(17)+e1*(b(18)+e1*(b(19)+e1*b(20))))+
     &e2*(b(21)+e1*(b(22)+e1*(b(23)+e1*(b(24)+e1*b(25))))))))

      return
      end
c*****************************************************************
```

Thesis
G828 Grigg
c.1 Far field wake velo-
city measurements with
hot film probes.